

Synthesis and Comparison of Transition Metal Complexes of Abnormal and Normal Tetrazolyliidenes: A Neglected Ligand Species

Lars-Arne Schaper,^{†,||} Xuhui Wei,^{†,||} Philipp J. Altmann,[†] Karl Öfele,[†] Alexander Pöthig,[†] Markus Drees,[†] János Mink,^{‡,§} Eberhardt Herdtweck,[†] Bettina Bechlars,[†] Wolfgang A. Herrmann,[†] and Fritz E. Kühn^{*,†}

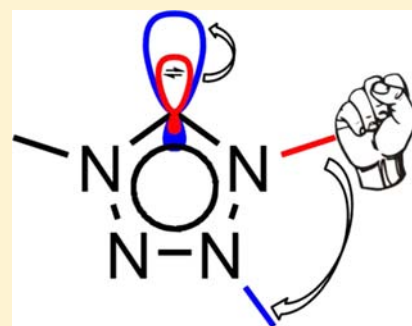
[†]Chair of Inorganic Chemistry/Molecular Catalysis, Catalysis Research Center, Technische Universität München, Ernst-Otto-Fischer-Str. 1, D-85747 Garching bei München, Germany

[‡]Research Institute of Chemical and Process Engineering, Faculty of Information Technology, University of Pannonia, H-8201 Veszprém, Hungary

[§]Institute of Molecular Pharmacology, Research Centre for Natural Sciences, Hungarian Academy of Sciences, H-1525 Budapest, Hungary

S Supporting Information

ABSTRACT: To date, only few examples of tetrazolylidene carbenes coordinated to transition metal complexes have been described. A direct comparison of “normal” tetrazolyliidenes (1,4-substitution pattern) and “abnormal” tetrazolyliidenes (also referred to as “mesoionic carbenes”; 1,3-substitution pattern) has not been performed at all. In this work, we describe coordination of both ligand types to a row of transition metals. For example, the first examples of tetrazolylidene Mo, Ag, or Ir complexes have been isolated and fully characterized. The mesoionic tetrazolylidene Ag compound **2d** is shown to be a viable carbene transfer reagent. By means of NMR, IR, and Raman spectroscopy, as well as X-ray crystallography and computational results, the pronounced differences between the two ligand substitution patterns are highlighted. It is shown that simply changing the position of a methyl group from N3 to N4 in the heterocycle can cause enormous differences in ligand characteristics.



INTRODUCTION

Since their first synthesis,¹ N-heterocyclic carbenes (NHCs) raised interest in the scientific community.² Most notably, discovery of their potential as valuable ligands in homogeneous catalysis³ led to a surge of research on this topic.⁴ The discovery of abnormal binding NHC ligands⁵ led to increased interest in donor strength variation of imidazolyliidenes and related systems.⁶ However, it was recently found that in the case of 1,2,3-triazolyliidenes variation between “abnormal” and “normal” ligand substitution patterns does not effectuate pronounced differences in donor capabilities.⁷ On the basis of this discussion, we were interested whether in the case of tetrazolyliidenes variation between normal and abnormal substitution pattern (Figure 1) would bring an effect on σ -donor abilities of the ligands.

Although this area is still somewhat underexplored to date, both types of substitution patterns were early reported for tetrazolylidene ligands bound to Fe carbonyl complexes.⁸ In more recent research, the donor properties of tetrazolylidene ligands with normal 1,4-substitution pattern were examined for Rh and Cr complexes.⁹ Catalytic application in hydroformylation of 1-octene was tested and a tetrazolylidene Rh compound showed outstanding performance.¹⁰ Raubenheimer and co-workers described the first Au complexes of this ligand type.¹¹ But also advances in tetrazolylidene ligands with abnormal 1,3-substitution pattern were reported. After their

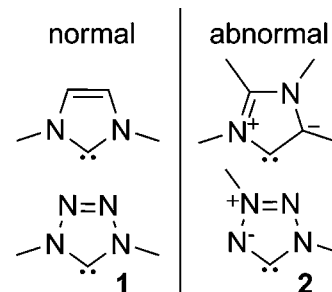


Figure 1. Imidazolylidene and tetrazolylidene ligands displaying normal and abnormal substitution pattern.

initial report on mesoionic tetrazolylidene complexes bound to Hg and Pd,¹² Araki and co-workers described decomposition studies of free carbene intermediates and coordination to Rh.¹³ Since to date no direct comparison between normal and abnormal tetrazolylidene ligands can be found, this report describes synthesis and detailed characterization of a variety of middle and late transition metals to provide an unrestricted overview of ligand properties evoked by a simple variation of substitution pattern. For this purpose, methyl groups as 1,4- or 1,3-substituents on the heterocycle were chosen to minimize

Received: March 3, 2013

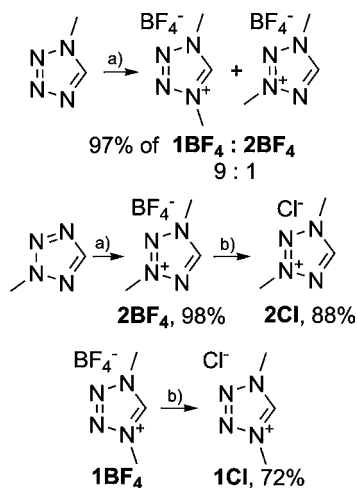
Published: May 24, 2013

their influence and restrict interaction with the coordination center. With spectroscopic, as well as computational means, it is attempted in this work to carve out the subtle distinctions between both ligand types.

RESULTS AND DISCUSSION

Synthesis of Tetrazolium Salt Precursors. The precursor for normal tetrazolylienes, 1,4-dimethyltetrazolium tetrafluoroborate (**1BF₄**), is synthesized by methylation of 1-methyltetrazole with trimethyloxonium tetrafluoroborate (Scheme 1).

Scheme 1. Synthesis of Ligand Precursor Salts^a



^aReaction conditions: (a) 1. 1.00 equiv of Me₃OBF₄, 0 °C, DCM, 2, RT, 1 h, DCM, 3. 40 °C, 10 min, DCM; (b) Cl⁻-charged ion exchange resin, H₂O.

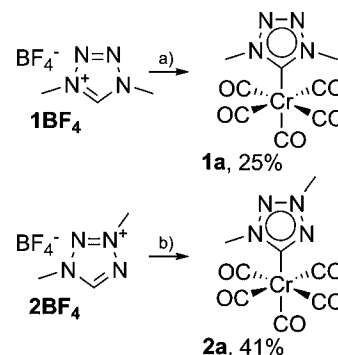
The reaction does not proceed cleanly, but typically affords a 95:5 mixture of **1BF₄** and the related 1,3-dimethyltetrazolium tetrafluoroborate (**2BF₄**), useful as precursor for abnormal carbenes. Changing the reaction conditions to lower temperatures (−78 °C) does not affect methylation selectivity. Clean samples of **1BF₄** can be obtained by recrystallization from ethanol (see Experimental Section). Since this method does not allow isolation of larger amounts of **2BF₄**, a different access route to the unsymmetrically substituted ligand precursor was chosen: Methylation of 2-methyltetrazole cleanly affords the 1,3-dimethyl product **2BF₄** in quantitative yields (Scheme 1).

Tetrafluoroborate anions in carbene precursor salts are not always suitable for carbene complex synthesis and often require additional reagents such as tetramethylammonium chloride. For this reason, advantage was taken of the water solubility of tetrafluoroborate precursors **1BF₄** and **2BF₄**, as the BF₄⁻ anion was exchanged with Cl⁻ by dissolving both compounds in water and subsequent passage through a Cl⁻ charged anion exchange resin. This anion exchange protocol gives 1,4-dimethyltetrazolium chloride (**1Cl**) and 1,3-dimethyltetrazolium chloride (**2Cl**) in good yields (Scheme 1). Both compounds are highly hygroscopic and have to be stored under argon after drying. Exothermic decomposition of **1BF₄** and **1Cl** can be observed in the presence of weak bases; therefore, careful handling is advised.

Synthesis of Normal and Abnormal Tetrazolyliene Complexes. The obtained tetrazolium salts can be applied in metal complex synthesis. Following a published route,^{9b} normal tetrazolyliene pentacarbonyl Cr complex **1a** can be synthe-

sized from **1BF₄** and K₃[Cr₂(CO)₆(μ-OH)₃] (Scheme 2). This compound was resynthesized in order to fully characterize and

Scheme 2. Synthesis of Cr Compounds **1a** and **2a**^a

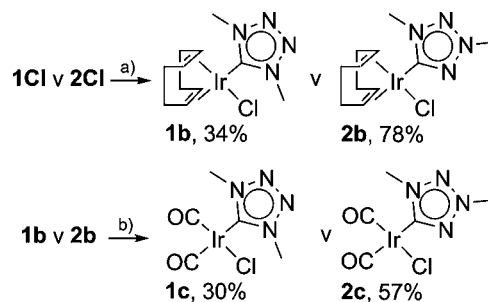


^aReaction conditions: (a) published procedure;^{9b} (b) 1. 0.60 equiv of Na₂[Cr₂(CO)₁₀], 10 min, H₂O, dried, 2. neat, 120 °C, vacuo.

compare it to compound **2a**, following an alternative route applying Na₂[Cr₂(CO)₁₀], on the basis of an earlier described synthesis for the related Fe complexes (Scheme 2).^{1a,8} Purification of both air and moisture stable compounds **1a** and **2a** is possible via column chromatography. ¹³C NMR quickly allows identification of both carbene species because of the characteristic carbene signals (190.3 ppm for **1a** and 200.9 ppm for **2a**) and furthermore because of the two carbonyl resonances each (in an intensity ratio of ~1:4 at around 210 ppm). FAB-MS further confirms the existence of **1a** and **2a** by giving the corresponding peaks for [M]⁺ in both cases. In addition, for both compounds clean elemental analyses were obtained.

For comparison of the two tetrazolyliene ligands' donor strengths, the corresponding Ir carbonyl compounds were synthesized, employing a convenient access route, just as in the case of **1a**, based on a metal precursor with internal base, [Ir(COD)(OMe)]₂. To avoid additional reagents (such as tetramethylammonium chloride) for the synthesis of [Ir(COD)Cl(tetraz)] compounds, tetrazolium chloride salts **1Cl** and **2Cl** were used. Reaction in acetone at RT overnight smoothly affords the Ir complexes **1b** and **2b** (Scheme 3). FAB-MS, as well as ESI-MS, suggest the existence of **1b** and **2b** (For **1b**, FAB-MS [M]⁺, [M-tetraz]⁺; ESI-MS [M - Cl + MeCN]⁺; for **2b**, FAB-MS [M]⁺; ESI-MS [M + 2H]²⁺), to the best of our knowledge the first examples of tetrazolyliene Ir complexes.

Scheme 3. Synthesis of Ir Complexes with Normal and Abnormal Tetrazolylienes^a

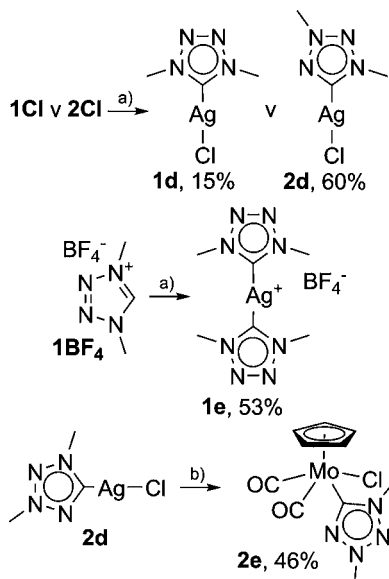


^aReaction conditions: (a) 0.5 equiv of [Ir(COD)(OMe)]₂, RT, 16 h, acetone; (b) CO (excess), 0 °C, 30 min, toluene or DCM.

Isolation of **1b** and **2b** is further evidenced by ^{13}C NMR (carbene resonances at 179.0 ppm and 186.8 ppm, respectively). The compounds were further analyzed by elemental analysis (see Experimental Section). In solution, both compounds are sensitive to air and moisture. The corresponding carbonyl complexes **1c** and **2c** can be synthesized by bubbling carbon monoxide through toluene or DCM solutions of the respective $[\text{Ir}(\text{COD})\text{Cl}(\text{tetrz})]$ complexes at 0 °C (Scheme 3). During the synthesis of **1c**, color change of the DCM reaction solution can be observed, indicating product decomposition. Nevertheless, once isolated, compounds **1c** and **2c** are sufficiently stable for analysis. ^{13}C NMR confirms the replacement of the COD ligand, since instead of COD resonances, new carbonyl signals can be observed (for **1c**, CO-signals at 180.4 and 167.6 ppm, carbene resonance at 173.1 ppm; for **2c**, COs at 181.6 and 168.7 ppm, carbene at 182.1 ppm). The complexes were fully characterized by FAB-MS, CI-MS, and elemental analysis.

To date, tetrazolylidene Ag compounds have not been described in literature, although their potential as carbene transfer reagents could open a gateway to a plethora of new transition metal compounds. Therefore, it was decided to follow the known path toward Ag NHC complexes utilizing Ag_2O .¹⁴ Ag Cl complexes **1d** and **2d** can be generated from tetrazolium salts **1Cl** and **2Cl** (Scheme 4). It should be noted,

Scheme 4. Synthesis of Tetrazolylidene Ag Complexes 1d, 2d, and 1e and Carbene Transfer Reaction Yielding 2e^a



^aReaction conditions: (a) Ag_2O , RT, 4 h, MeCN; (b) 0.90 equiv of $[\text{Mo}(\text{CO})_3\text{ClCp}]$, 40 °C, 5 h, DCM.

that intense exothermic decomposition reactions under smoke formation were observed when allowing contact between solid **1Cl** and solid Ag_2O under air. Therefore, it is mandatory to use thoroughly dried **1Cl** and to charge reagents into separate flasks in the glovebox for this reaction. Nevertheless, normal tetrazolylidene complex **1d** was only isolated in very low yields, certainly attributable to the ligand's tendency to release nitrogen in the presence of bases^{8b}: **1d** was even decomposing as solid within days under Argon at room temperature. For these reasons, the Ag complex was only characterized by ^1H NMR, as well as FAB-MS. Abnormal tetrazolylidene compound

2d, however, can be isolated in higher yield and proves to be more stable. A characteristic carbene resonance can be observed in ^{13}C NMR at 182.4 ppm and gives evidence for the isolation of **2d**. Further proof of carbene formation was found in FAB-MS, as well as elemental analysis. Finally, X-ray crystallographic data satisfactorily prove the structure of **2d**, as shown in Scheme 4. Interestingly, another alternative of a normal tetrazolylidene Ag complex (**1e**) can be synthesized by using **1BF4** as ligand precursor and Ag_2O as metal source. Also this compound suffered from lowered stability, which prevented us from obtaining a suitable elemental analysis. X-ray crystallography confirmed the structure suggested in Scheme 4. The limited stability of the compounds with 1,4-substitution patterns supposedly arises from their tendency to release nitrogen from the backbone, as was earlier observed.¹⁵

Ag complex **2d** was tested in the carbene transfer reaction with Mo precursor $[\text{Mo}(\text{CO})_3\text{ClCp}]$.¹⁶ The transfer of the abnormal tetrazolylidene ligand to Mo proceeds successfully, as proven by the isolation of complex **2e**. ^1H NMR shows a slightly shifted Cp ligand signal (from 5.66 ppm to 5.61 ppm). Also ^{13}C NMR suggests formation of **2e** by revealing two carbonyl signals of the same intensity (at 260.5 ppm and 253.2 ppm) and a carbene resonance at 196.7 ppm. Furthermore, the new compound's IR spectrum displays pronounced differences compared with the precursor's carbonyl absorption bands (1964 and 2056 cm^{-1} in $[\text{Mo}(\text{CO})_3\text{ClCp}]$; 1940 and 1844 cm^{-1} in **2e**). Finally, FAB-MS, X-ray diffraction spectroscopy and elemental analysis prove existence of **2e**.

Spectroscopic Studies. To further understand the electronic differences between abnormal and normal tetrazolylidene ligand systems, NMR spectroscopy provides interesting potential to estimate ligands' donor strength. While it became obvious that the ^{13}C NMR carbene resonance of various NHCs cannot be used as reliable probe for determination of NHC ligands' donor strength,^{9a,17} it has been shown that NMR signals of metal coordinated olefins directly correspond to varying electron donor capacities of the other coordinated moieties.¹⁸ Stronger electron-donating ligands increase the electron density at the metal center, which in turn leads to increased metal-to-olefin back-bonding with intensified structural resemblance of a metalla-cyclopropane. This enhanced alkyl character of the olefin ligand is well observable in ^{13}C NMR by upfield shift of the carbon resonances. For this reason, we compared the ^{13}C NMR chemical shifts obtained for the olefinic carbons in the COD ligands of complexes **1b** and **2b** (Figure 2). While the COD signals of the two compounds at around 53 ppm in the spectrum do not show any remarkable differences (53.83 ppm for **1b** and 53.68 ppm for **2b**), the low-field COD signals highlight distinct variation (87.70 ppm for **1b** and 85.11 ppm for **2b**, see Figure 2), which implies that in the abnormal tetrazolylidene Ir compound **2b** higher electron density is present at the Ir center.

Vibrational spectroscopy of carbonyl substituted transition metal complexes is a viable experimental method for assessing the donor strength of various ligands.^{9a,17a,19} The recorded IR spectra, as well as the Raman spectra of the Cr complexes **1a** and **2a**, show pronounced differences in the carbonyl stretching frequencies (recorded in solid state). A trend can be identified, as in most cases the carbonyl stretching frequencies for compound **2a** are lower than for **1a**, suggesting increased σ -donor strength of the abnormal tetrazolylidene ligand in **2a**. In the case of metal carbonyls, the Raman spectroscopy allows for even better distinction between the carbonyl bands (because of

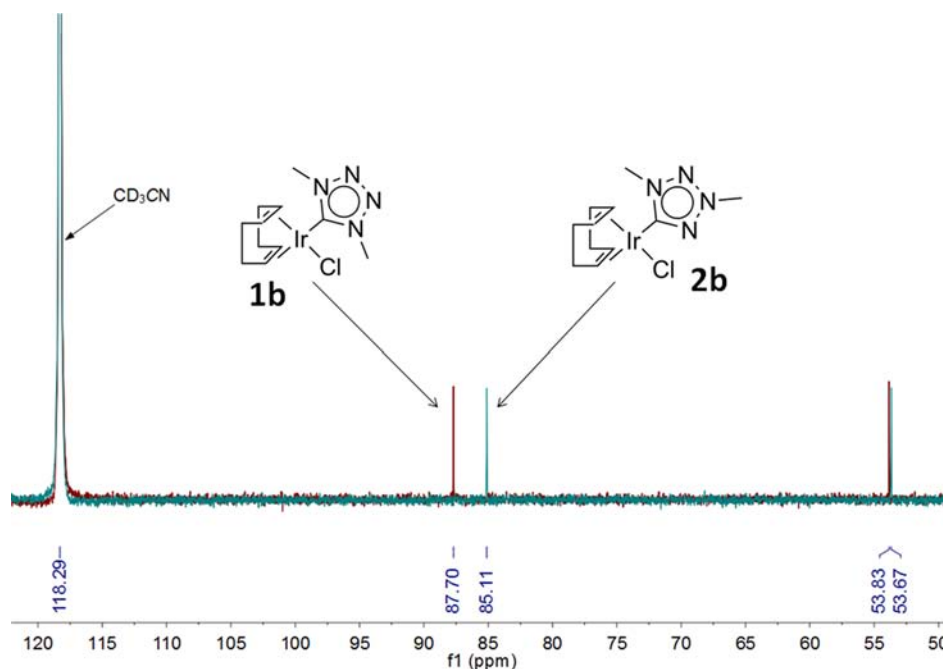


Figure 2. Superimposed ^{13}C NMR spectra of **1b** and **2b**, showing section between 50 and 120 ppm. The increased electron density at the metal center in **2b** leads to an upfield shift of the COD signal highlighted by the arrows.

the narrow natural band widths) and supports the observed general trend of enhanced electron density on the metal center of **2a** (see spectra in Figure 3, observed wavenumbers and tentative assignments in Table 1).

For example, the CO stretching bands for the A_1 axial vibration are clearly lowered in **2a** (IR, 1910 cm^{-1} ; Raman, 1909 cm^{-1}) compared to **1a** (IR, 1925 cm^{-1} ; Raman, 1930 cm^{-1}). Furthermore, strong differences can be observed in comparison of the E (eq) stretching IR bands in **2a** (IR, 1882 cm^{-1}) and in **1a** (IR, 1891 cm^{-1}), and still well detectable difference is in axial CO stretching, which Raman features at 1901 and 1888 cm^{-1} for **1a** and **2a** complexes, respectively.

Corresponding with the observations of the C–O bond stretching vibrations, the CrC stretch frequencies (474 , 460 , 408 , and 397 cm^{-1}) are higher in **2a** than in **1a** (468 , 454 , 400 , and 392 cm^{-1}), suggesting higher metal to CO ligand back-bonding and resulting higher Cr–C bond strength in abnormal tetrazolylidene substituted compound **2a** (see Table 1). Based on the observed wavenumbers, C–O bond stretching force constants as well as stretch–stretch interaction terms between the CO stretching coordinates were calculated, according to the Effective G-Matrix Method (EGM) described elsewhere (Table 2).²⁰ For the equatorial CO ligands, a force constant of 15.22 N cm^{-1} was calculated for **1a** and 15.13 N cm^{-1} for **2a**. For the axial CO ligand, force constants of 14.37 N cm^{-1} for **1a** and 14.17 N cm^{-1} for **2a** were obtained. Yet again, these values suggest higher electron donor strength in ligand **2a**, since a lowered C–O bond force constant is a result of increased metal to ligand back-bonding interactions.

Standard compounds for assessing σ -donor strengths of NHC ligands are Rh and Ir NHC carbonyl complexes [(NHC)(CO) $_2$ MCl].^{9a,17a} The average of the IR carbonyl bands is $\nu(\text{CO})_{\text{av}} = 2032.5\text{ cm}^{-1}$ in **1c** and $\nu(\text{CO})_{\text{av}} = 2022\text{ cm}^{-1}$ in **2c**, corresponding to a $\nu(\text{TEP}) = 2057.7\text{ cm}^{-1}$ for **1c** and $\nu(\text{TEP}) = 2048.8\text{ cm}^{-1}$ in **2c** (both measured in DCM). Again, the increased electron donation caused by the abnormal 1,3-substitution pattern in **2c** can be observed. The calculated

$\nu(\text{TEP})$ values allow for classifying the σ -donor strength of the normal 1,4-substituted tetrazolylidene ligand **1** in the area of P(iPr) $_3$, one of the weakest values obtained for NHCs to date, while the electron donation ability of abnormal 1,3-substituted tetrazolylidene ligand **2** corresponds quite well to the one observed for ItBu.^{2h} The observed similarity between abnormal tetrazolylidene ligand **2** and normal imidazolylidene is reflected in the IR bands measured for Mo carbonyl compound **2e**. Recently, Hor et al. synthesized a similar compound coordinated to dibenzyl-imidazolylidene [Mo(CO) $_2$ Cl(IBz)]. The IR stretching frequencies for the carbonyl moieties in **2e** (1940 cm^{-1} and 1844 cm^{-1} , measured in solid state) are considerably lower than the values observed in Hor's compound [1953 and 1872 cm^{-1} (KBr)],¹⁶ suggesting higher electron density donated by the abnormal tetrazolylidene ligand.

Electrochemical Studies. In addition, it is interesting to know whether the different substitution patterns have an effect on the molecular dipole moment of both Cr complexes. Therefore, dipole measurements were performed in benzene solutions of both compounds. For **1a**, a value of $3.7 \pm 0.1\text{ D}$ and for **2a** a value of $7.96 \pm 0.1\text{ D}$ was found (for comparison, the dipole moment of 1,3-dimethylimidazolylidene Cr(CO) $_5$, which was also measured, is $7.00 \pm 0.1\text{ D}$). These values and comparison to the imidazolylidene complex suggest that in the case of the newly described compounds electronic influences dominate over steric effects on the dipole moment. The experimentally obtained values were compared to values obtained from the DFT calculations of these complexes (vide infra). For the normal 1,4-dimethyltetrazolylidene complex **1a**, a value of 3.37 D was found, while for abnormal 1,3-dimethyltetrazolylidene complex **2a** a dipole moment of 9.02 D was obtained, suggesting good accordance with experimental values.

Crystallographic Studies. Single crystals suitable for X-ray crystallography of both Cr compounds **1a** and **2a** could be grown by slow evaporation of hexane solutions of the respective

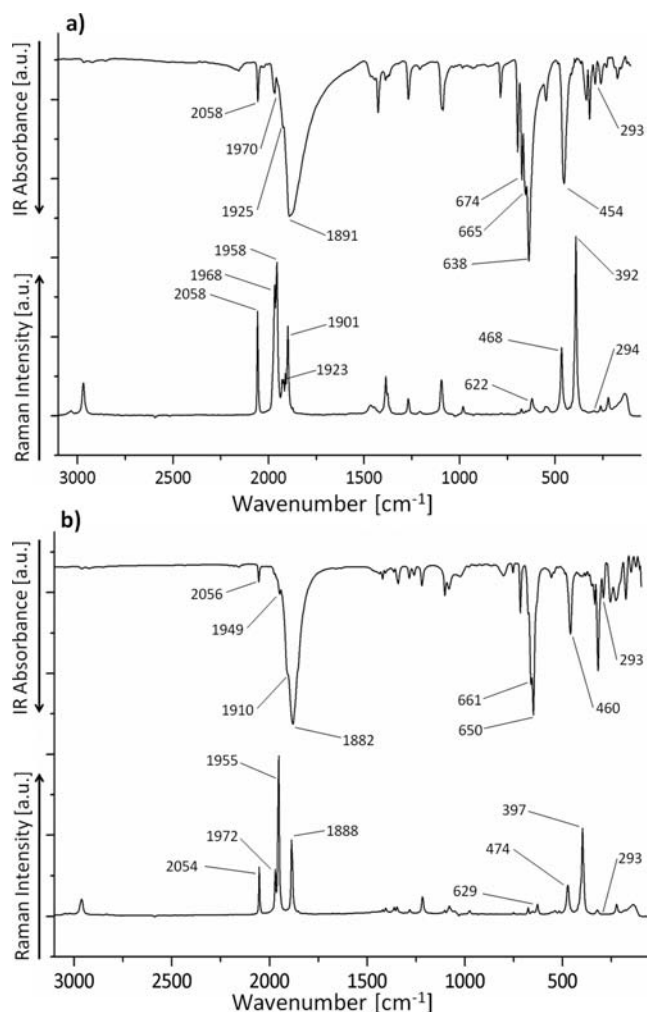


Figure 3. Infrared-, far-infrared (upper traces), and Raman-spectra (lower traces) of Cr compounds **1a** (a) and **2a** (b), recorded in solid state.

compounds. Both compounds display an almost ideal orthogonal structure (Figure 4), in which the angles between the carbene carbon, the Cr center and the cis-carbonyl ligands display an angle close to ideal 90° [for example C1–Cr1–C5 $93.13(9)^\circ$ for **1a**; C8–Cr1–C1 $95.89(8)^\circ$ for **2a**].

This observation is substantiated by the observed angle between the carbene carbon, the Cr center and the trans carbonyl ligand, which is close to ideal 180° [C5–Cr1–C8 $176.24(9)^\circ$ for **1a** and C1–Cr1–C4 $176.54(9)^\circ$ for **2a**]. These values are parallel to earlier observations from our group for the corresponding dimethyl-imidazolylidene compound.²¹ The two methyl groups bound to the carbene-neighbor nitrogen in **1a** seem to give rise to a higher torsion angle for C4–Cr1–C5–N1 [$45.0(2)^\circ$] as in **2a** [C8–Cr1–C1–N1 $29.9(2)^\circ$], certainly attributable to steric factors. When comparing the carbene-metal bond lengths, significant differences can be observed: the carbene–Cr bond lengths in both tetrazolylidene compounds [**1a** Cr1–C5 $2.096(2) \text{ \AA}$, **2a** $2.0958(19) \text{ \AA}$] are shorter than in the methyl-imidazolylidene example presented by our group [$2.138(2) \text{ \AA}$] or for the pyrazolylidene example in the same publication [$2.1327(4) \text{ \AA}$].²¹ Comparing our results with other carbene–chromium bond lengths of similar compounds described in literature,²² no equally short distances were found — distances range from $2.125(4)$ ^{22c} to $2.264(4) \text{ \AA}$

for Arduengo's extraordinary example with phosphoryl substituted backbone.^{22f} These observations might be explained by an increased amount of π -contributions to the carbene metal bond facilitated by the four nitrogens in the ligand's heterocycle (see computational part).

Single-crystals suitable for X-ray diffraction of the Ir compound **1b** were grown by slow evaporation of a saturated DCM solution of the complex. Crystals of **2b** were grown by layering a saturated acetone solution of **2b** with hexane and cooling of this solvent mixture overnight at 4°C . Both compounds exhibit a close to ideal square planar structure, which can be deduced from the Cl1–Ir1–C1 angle [$89.92(8)^\circ$ for **1b** and $90.34(10)^\circ$ for **2b**] (Figure 5). As observed in other imidazolylidene carbene Ir COD structures,^{5c,23} also here the torsion angles for [Cl1–Ir1–C1–N1 $79.8(3)^\circ$ in **1b** and Cl1–Ir1–C1–N1 $74.2(3)^\circ$ in **2b**] highlight that the ligand plane is twisted almost completely perpendicular to the coordination plane. This twist can certainly be explained by steric reasons. The carbene Ir bond lengths [**1b** $2.012(3) \text{ \AA}$, **2b** $2.027(3) \text{ \AA}$] are in the range of usual imidazolylidene Ir bond lengths in structures published by us or other groups [bond lengths in these examples range from $2.018(4)$ to $2.069(6) \text{ \AA}$].^{5c,23} The spectroscopic section showed that the olefinic COD signals observable in ^{13}C NMR vary with the electron density at the metal center and hence the electron donor strength of the ligand, because of the increased metallacyclopropane character in the Ir–COD bonding situation.^{18a} We were curious, whether these spectroscopic observations were reflected in the crystal structures of compounds **1b** and **2b**. Extending this theory, the bond lengths of the COD double bonds should be slightly elongated when electron density is increased. Indeed, a slight trend is observable, as the olefinic bond lengths are in average somewhat shorter in the normal tetrazolylidene complex in comparison to the abnormal tetrazolylidene compound [**1b** C4–C5 $1.411(4) \text{ \AA}$, C8–C9 $1.381(4) \text{ \AA}$, average 1.396 \AA ; **2b** C4–C5 $1.392(5) \text{ \AA}$, C8–C9 $1.429(5) \text{ \AA}$, average 1.4105 \AA]. The Ir COD complex bound to a stronger electron donating abnormal imidazolylidene, described by Crabtree and co-workers, even shows slightly more elongated olefinic bond lengths (C20–C21 $1.418(13) \text{ \AA}$, C25–C24 $1.41(2) \text{ \AA}$, average 1.414 \AA).^{5c} Although it must be noted that these values cannot be described as significant (they only differ within the standard deviation obtained for the measurements), their trend suggests a reduced donor strength for the normal tetrazolylidene ligand **1** yet again.

For X-ray crystallography of Ir carbonyl compound **2c**, suitable single-crystals were grown by slow diffusion of pentane into a saturated toluene solution of the complex. The molecular structure of **2c**, depicted in Figure 6, shows a typical square planar geometry, as can be deduced from the angles Cl1–Ir–C1 [$87.35(11)^\circ$] and C1–Ir1–C4 [$177.90(16)^\circ$]. As observed for the Cr complexes **1a** and **2a**, the carbene metal bond [Ir1–C1 $2.062(4) \text{ \AA}$] is shortened in comparison to metal bonds in other imidazolylidene complexes or 1,2,3-triazolylidene complexes: Ir–carbene bond distances range from $2.0714(4)$ to $2.121(14) \text{ \AA}$ for a variety of seven imidazolylidene complexes reported by Nolan and co-workers,^{17a} and for 1,2,3-triazolylidenes bond lengths of $2.070(5)$ or $2.098(8) \text{ \AA}$ were reported.^{6a,7} Again, the ligand is twisted out of the coordination plane, as shown by a torsion angle for Cl1–Ir1–C1–N1 of $62.7(3)^\circ$.

The crystal structure of Ag complex **2d** (crystals grown from slow diffusion of diethyl ether into a saturated MeCN solution

Table 1. Observed Vibrational Wavenumbers (cm^{-1}) and Tentative Assignments

1a, [Cr(1,4-dime-tet)(CO) ₅]		2a, [Cr(1,3-dime-tet)(CO) ₅]		tentative assignment
IR ^a	Raman ^a	IR ^a	Raman ^a	
2058(28)	2058(67)	2056(12)	2054(30)	CO str, A ₁ (eq)
1970(22)	1968(85)	1976(7)	1972(30)	CO str, B ₁ (eq)
	1958(100)	1968(8)sh	1955(100)	
1925(44)sh	1930(22)	1949(19)	1909(8)	CO str, A ₁ (ax)
	1923(22)	1910(68)sh		
	1913(27)		1888(47)	
	1901(58)		1880(30)sh	CO str, E(eq)
1891(100)		1882(100)	1854(3)	
1870(95)sh	1874(4)	1854(60)sh	1854(3)	
674 (75)	677(4)	677(15)	675(4)	Cr(CO) def(A ₁)
665(85)	654vw, 642vw	661(75)	652vw	Cr(CO) deg (E)
638(120)		650(94)		
	622(10)	630(25)sh	629(6)	
548(25)	546(5)b	557(7)	554vw	Cr(CO) def (E)(eq)
	538(5)	543(5)	539(2)	Cr(CO) def s (B ₁)(eq)
			518(2)	
485(1)	468(44)	488(5)	474(19)	CrC str (A ₁)(trans)
454(78)		460(44)		CrC str (E) (eq)
	400(40)sh		408(20)sh	CrC str (B ₁)(eq)
	392(117)		397(54)	CrC str (A ₁)(eq)
293(17)	294(0.2)	293(16)	297(0.7)	CrC _{carbene} str

^aBand intensities are normalized to 100 arbitrary intensity units and presented in brackets: sh = shoulder, vw = very weak, b = broad. Italic wavenumbers exhibit 100 relative intensity units. Multiple bands are due to the solid state splitting. The strongest CO stretching bands were selected for simplified force constants calculation.

Table 2. Selected Experimental CO Stretching Frequencies (cm^{-1}), Calculated CO Stretching Force Constants (N cm^{-1}), and Stretch–Stretch Interaction Force Constants (N cm^{-1})

species	1a	2a
A ₁ (eq)	2058	2055
A ₁ (ax)	1901	1888
B ₁ (eq)	1958	1955
E(eq)	1891	1882
	force constant	
f_c	15.22	15.13
f_a	14.37	14.17
$f_{cc}(\text{cis})$	0.32	0.31
$f_{cc}(\text{trans})$	0.84	0.88
f_{ca}	0.24	0.25

of the complex, Figure 5) exhibits a bent linear geometry, with the Cl1–Ag1–C1 angle [$167.82(6)^\circ$] clearly deviating from the ideal 180° . However, this behavior is relatively common in NHC Ag Cl complexes, as shown by others.²⁴ Interestingly, complex **2d** forms a 2D coordination polymer in solid state through interaction of the Cl and Ag atoms of two formerly independent molecules, leading to a T-shaped structure [Ag1–Cl1a 2.9413(8) Å]. This finding corresponds well with a variety of described related polymeric or cluster structures, which were observed for NHC Ag complexes.^{2b} The metal–carbene bond distance of Ag1–C1 2.097(2) Å is not shorter than in other described imidazolylidene Ag Cl complexes; for example Nolan and co-workers observed Ag–C_{carbene} distances ranging from 2.056(6) to 2.121(1) Å.^{24c} Argentophilic interactions were not observed; instead the Ag center slightly interacts with ligands'

N2 from the upper and lower polymer layer (Ag–N2' 3.221(1) Å (symmetry code N2' 2 - x, 1/2 + y, 1 - z)).

Unfortunately, the quality of the single crystals grown for **1e** did not allow for accurate assignment of residual electron density because of a disordered BF_4^- anion; therefore, bond angles and distances cannot be discussed (Figure 8). For compound **2e**, single-crystals suitable for X-ray diffraction were grown by layering a saturated DCM solution of **2e** with hexane and cooling overnight at 4°C . **2e** exhibits the expected four legged piano-stool structure with unexceptional angles of $76.62(6)^\circ$ for Cl1–Mo1–C1 and $121.45(10)^\circ$ for C1–Mo1–C9 (Figure 9). For example, Hor et al. reported in the similar **IBz** substituted compound an angle of $77.26(9)^\circ$ for the angle between carbene and Cl.¹⁶ But the carbene Mo bond distance of 2.173(2) Å in **2e** is significantly shortened compared with the values in Hor's compound [2.221(3) Å]. This shortened distance could be a result of less steric hindrance of the abnormal tetrazolylidene when compared to the more spacious benzyl ligand.

Computational Studies. The pronounced differences between the two ligands caused us to further investigate the nature of the carbene–metal bond in tetrazolylidenes by means of theoretical considerations. Therefore, we compared **1a** and **2a** in terms of their electronic structure with two related normal and abnormal imidazolylidene complexes **nIMI** and **aIMI** (Table 4) by means of density functional theory (DFT). The normal imidazolylidene Cr compound **nIMI** was subject to earlier theoretical investigations by several groups.^{21,25} π -Back-bonding contributions to the NHC–metal bond were found in a variety of investigations,²⁶ also in the case of Cr NHC complexes.²⁷ Recently, a study on Au NHC complexes compared the bonding properties of abnormal and normal

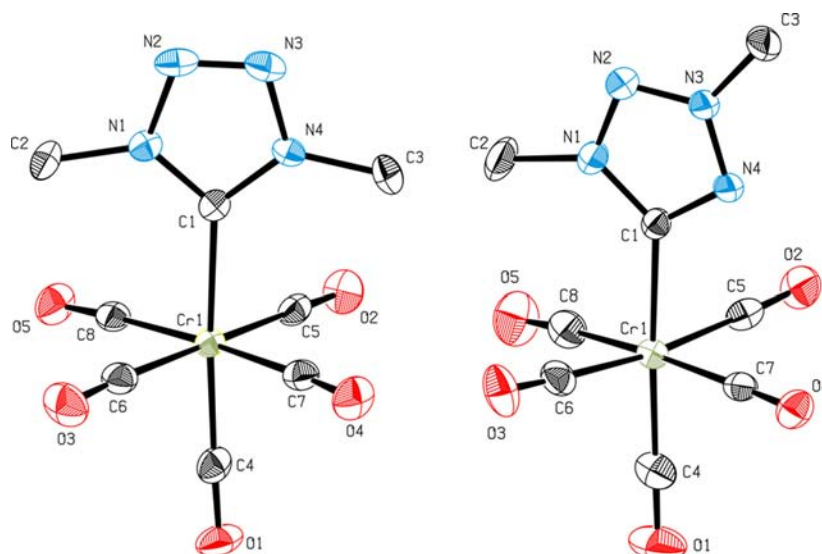


Figure 4. ORTEP style plot of compound **1a** (left) and **2a** in the solid state. Thermal ellipsoids are drawn at the 50% probability level. Hydrogen atoms are omitted for clarity. Selected bond distances [Å], angles [deg], and torsion angles [deg]: **1a** Cr1–C1 2.097(2), Cr1–C4 1.867(2), Cr1–C5 1.900(2), Cr1–C6 1.900(2), Cr1–C7 1.899(2), Cr1–C8 1.907(2), N1–C1–N4 100.20(16), C1–Cr1–C4 176.25(9), C1–Cr1–C5 88.85(9), C5–Cr1–C1–N1 129.63(19); **2a** Cr1–C1 2.096(2), Cr1–C4 1.869(2), Cr1–C5 1.903(2), Cr1–C6 1.910(2), Cr1–C7 1.896(2), N1–C1–N4 104.13(15), C1–Cr1–C4 176.54(9), C1–Cr1–C8 95.89(9), C5–Cr1–C1–N1: 118.87(18).

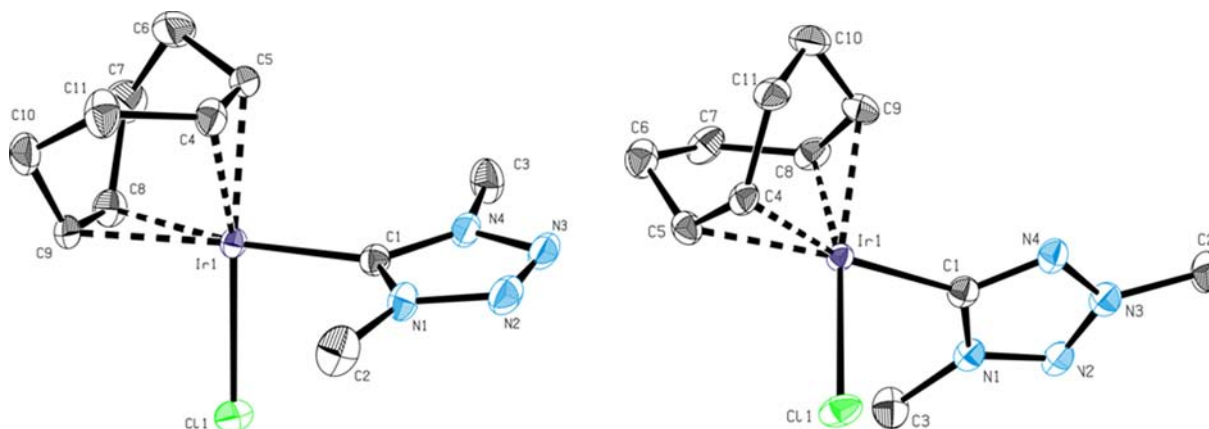


Figure 5. ORTEP style plot of compound **1b** (left) and **2b** in the solid state. Thermal ellipsoids are drawn at the 50% probability level. Hydrogen atoms are omitted for clarity. Selected bond distances [Å], angles [deg], and torsion angles [deg]: **1b** Ir1–C1 2.012(3), Ir1–Cl1 2.3583(7), C4–C5 1.411(4), C8–C9 1.381(4), Cl1–Ir1–C1 89.92(8), Cl1–Ir1–C1–N1 –79.8(3); **2b** Ir1–C1 2.027(3), Ir1–Cl1 2.3675(9), C4–C5 1.392(5), C8–C9 1.429(5), Cl1–Ir1–C1 90.34(10), Cl1–Ir1–C1–N1 74.2(3).

imidazolylienes and found π -backbonding in the case of the normal imidazolyliene to be the reason for higher stability of the carbene Au bond.²⁸

The four complexes depicted in Table 4 were calculated by the PBEPBE/6-31G* level of theory. Consistent with the observations made in X-ray crystallography, the calculated distances for both tetrazolyliene complexes were shorter than for the imidazolyliene congeners. However, the shortened distance in **2a** in comparison to **1a** contradicts our observations, just as the shortened distance of **aIMI** in comparison to **nIMI** contradicts the observations of others.²⁸ These slight deviations can be explained by the somewhat heightened steric demand of **1a** and **nIMI** in comparison to the other two compounds (control calculations of structures with hydrogens replacing the ligands' methyl groups gave the anticipated succession of distances, see Supporting Information). The Mulliken charges on the carbene carbon obtained from calculation of the free carbenes reflect the estimated σ -donor strengths of the ligands

to decrease in the order of **aIMI** > **2a** > **nIMI** > **1a**. The ligand bond energies (LBE) allow a good comparison of the donor strength of the carbenes in metal complexes. Carbene **aIMI** has the strongest bond energy with 67.4 kcal/mol, while the lowest LBE has been calculated for **1a** (55.7 kcal/mol). According to the assumption that the stronger donor has the most exothermic LBE (or in other words needs the highest energy to break the ligand–metal bond) this trend for the donor strength of these ligands should have the order **aIMI** > **2a** > **nIMI** > **1a**. According to Koopman's Theorem, HOMO energies should follow the tendency of the ionization potentials of the respective compounds ($IP = -\epsilon(\text{HOMO})$). The calculated HOMO energies of the free carbenes and the Cr complexes suggest that compound stability toward ionization decreases with decreasing donor strength of the ligands, except for the HOMO energies (all HOMOs represent the lone pair of the carbene carbon) of **2a** and **nIMI**, which show an opposite trend. When comparing the HOMO energies of the complexes,

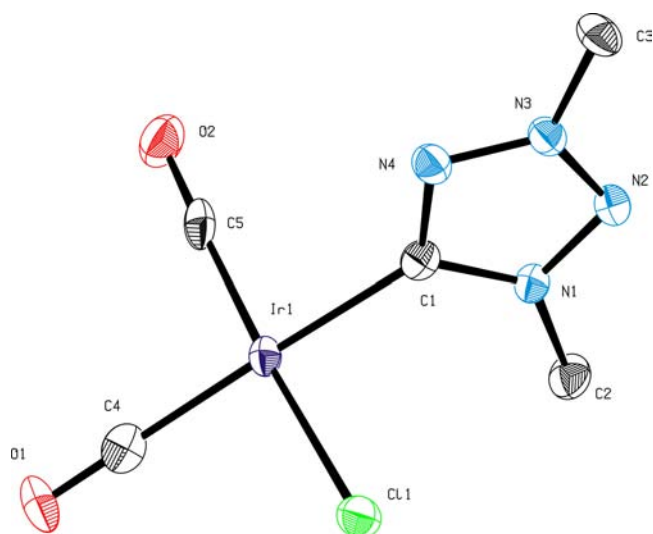


Figure 6. ORTEP style plot of compound **2c** in the solid state. Thermal ellipsoids are drawn at the 50% probability level. Hydrogen atoms are omitted for clarity. Selected bond distances [Å], angles [deg], and torsion angles [deg]: Ir1–C1 2.062(4), Ir–Cl1 2.3490(9), Ir–C4 1.902(4), Ir–C5 1.832(4); Cl1–Ir–C1 87.35(11), C1–Ir1–C4 177.90(16); Cl1–Ir1–C1–N1 62.7(3).

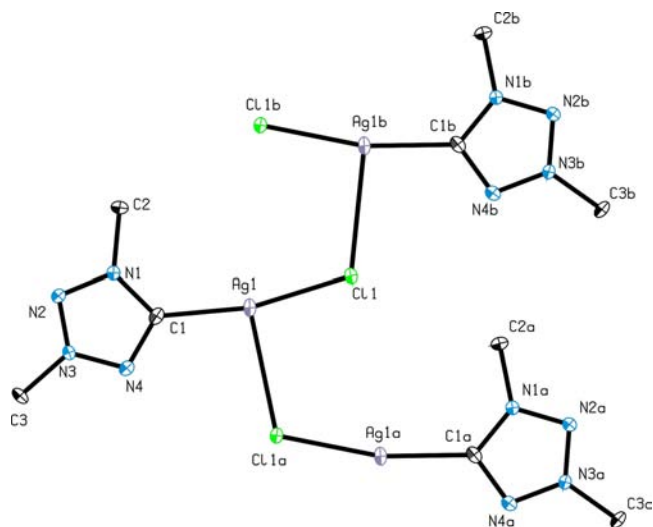


Figure 7. ORTEP style plot of compound **2d** in the solid state. Thermal ellipsoids are drawn at the 50% probability level. Hydrogen atoms are omitted for clarity. Selected bond distances [Å] and angles [deg]: Ag1–C1 2.097(2), Ag1–Cl1 2.3797(7), Ag1–Cl1a 2.9413(8), Cl1–Ag1–C1 167.82(6).

then **aIMI** shows the lowest ionization potential, while **1a** shows the highest. **2a** and **nIMI** are in between and almost at the same value.

To examine the four calculated complexes for evidence of the ligands' π -acceptor capabilities, a fragment orbital analysis of the NHC and $\text{Cr}(\text{CO})_3$ for all complexes was undertaken. For these investigations, the z -axis was defined as Cr–NHC coordination axis (Figure 10).

The calculated electron populations of the NHC and Cr fragments, as well as the populations in the complex orbitals were compared. Upon coordination of the ligand, an increase in electron population should be observable at least in the d -orbitals of the coordination axis. This observation could be

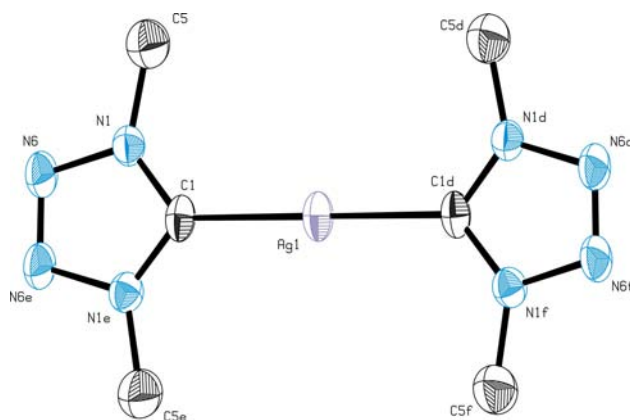


Figure 8. Ortep drawing (50% probability) of the cationic complex of compound **1e** as structural proof. Since the BF_4^- anion is located on a special position, the strong disorder could not be resolved adequately and no further parameters are discussed.

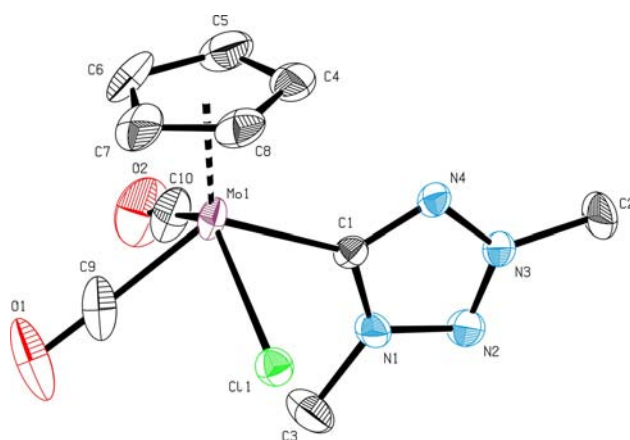


Figure 9. ORTEP style plot of compound **2e** in the solid state. Thermal ellipsoids are drawn at the 50% probability level. Hydrogen atoms are omitted for clarity. Selected bond distances [Å] and angles [deg]: Mo1–C1 2.173(2), Mo1–Cl1 2.5206(6), Mo1–C9 1.961(3), Mo1–C10 1.952(3), Cl1–Mo1–C1 76.62(6), C1–Mo1–C9 121.45(10).

made, as the change in electron population in the Cr $d_{x^2-y^2}$ -orbital went parallel to the estimated σ -donor strengths (Figure 10). In contrast, a higher gain in electron population could be observed in the Cr d_{z^2} - and s -orbital with decreasing donor strength. However, when stepping back from this rather constrained view of the complexes, it becomes obvious that the missing electron density in the case of the stronger electron donating ligands is donated to the carbonyl acceptor ligands, as reflected in the calculated IR vibrational bands [$\nu(\text{IR-average}) = \text{aIMI } 1979.1$, **2a** 1990.8, **nIMI** 1982.4, **1a** 1991.8]. When examining the other d -orbitals of the complex for evidence of metal to carbene backbonding, a decrease in electron population in the d_{xz} - and d_{yz} -orbitals of Cr suggested a backbonding contribution of the metal and revealed an increase in Cr–carbene back-bonding in the sequence of **aIMI** < **2a** < **nIMI** < **1a** (Figure 11a).

Apart from the Cr orbitals, also suitable p -orbitals of the carbene carbon were investigated for increased π -bonding contributions. Since the p_z -orbital participates in the σ -bond to the metal, the p_x - and p_y -orbitals of the carbene carbon should be examined in isolation. While for both abnormal NHC complexes **aIMI** and **2a** only a negligible increase in electron

Table 3. Crystallographic Data for Compounds 1a, 1b, 2a, 2b, 2c, 2d, and 2e

	1a	1b	2a	2b	2c	2d	2e
formula	C ₈ H ₆ CrN ₄ O ₅	C ₁₁ H ₁₈ ClIrN ₄	C ₈ H ₆ CrN ₄ O ₅	C ₁₁ H ₁₈ ClIrN ₄	C ₅ H ₆ ClIrN ₄ O ₂	C ₃ H ₆ AgClN ₄	C ₁₀ H ₁₁ ClMoN ₄ O ₂
fw	290.17	433.96	290.17	433.96	381.81	241.44	350.62
color/habit	colorless/fragment	yellow-orange/fragm.	colorless/fragment	yellow-orange/fragm.	colorless/fragment	yellow/block	red-orange/fragment
cryst dimensions (mm ³)	0.08 × 0.14 × 0.28	0.31 × 0.32 × 0.39	0.12 × 0.15 × 0.32	0.07 × 0.13 × 0.29	0.09 × 0.18 × 0.19	0.04 × 0.10 × 0.12	0.19 × 0.19 × 0.31
cryst syst	orthorhombic	monoclinic	monoclinic	monoclinic	monoclinic	orthorhombic	tetragonal
space group	<i>Fdd2</i> (No. 43)	<i>P2₁/c</i> (No. 14)	<i>P2₁/n</i> (No. 14)	<i>P2₁/c</i> (No. 14)	<i>P2₁/n</i> (No. 14)	<i>Pnma</i> (No. 62)	<i>P4/n</i> (No. 85)
<i>a</i> (Å)	26.4751(8)	16.6456(4)	12.0361(10)	16.2176(5)	8.9809(2)	6.9900(12)	19.9942(2)
<i>b</i> (Å)	28.2602(9)	7.2230(2)	7.4686(6)	6.7070(2)	7.9092(2)	6.3339(12)	19.9942(2)
<i>c</i> (Å)	6.2479(2)	11.3038(3)	13.5986(10)	12.0627(4)	13.9153(3)	15.124(3)	7.4709(1)
α (deg)	90	90	90	90	90	90	90
β (deg)	90	105.001(1)	103.003(4)	93.949(1)	99.3855(10)	90	90
γ (deg)	90	90	90	90	90	90	90
<i>V</i> (Å ³)	4674.6(3)	1312.75(6)	1191.07(16)	1308.96(7)	975.20(4)	669.6(2)	2986.63(7)
<i>Z</i>	16	4	4	4	4	4	8
<i>T</i> (K)	123	123	123	123	123	100	123
<i>D</i> _{calcd} (g cm ⁻³)	1.649	2.196	1.618	2.202	2.601	2.395	1.559
μ (mm ⁻¹)	0.998	10.358	0.980	10.388	13.939	3.318	1.056
<i>F</i> (000)	2336	824	584	824	696	464	1392
θ range (deg)	2.11–25.37	2.53–25.39	2.04–25.32	3.29–25.36	2.52–25.36	2.69–25.45	1.44–25.36
index ranges (<i>h, k, l</i>)	±31, –34 – 33, –7, –6	±20, ±8, ±13	±14, ±8, ±16	–11, –19, ±8, ±14	±10, ±9, ±16	±8, ±7, ±18	±24, ±24, ±9
no. rflns collected	16739	31732	15388	14710	24705	14994	64066
no. indep rflns/ <i>R</i> _{int}	1990/0.034	2408/0.030	2162/0.040	2369/0.037	1784/0.067	682/0.0487	2736/0.0411
no. of obsd rflns (<i>I</i> > 2 σ (<i>I</i>))	1881	2257	1857	2239	1740	655	2428
no. data/restraints/params	1990/1/165	2408/0/156	2162/0/187	2369/0/156	1784/0/121	682/8/65	2736/0/165
<i>R</i> ₁ / <i>wR</i> ₂ (<i>I</i> > 2 σ (<i>I</i>)) ^a	0.0214/0.0492	0.0136/0.0300	0.0268/0.0630	0.0185/0.0440	0.0175/0.0444	0.0123/0.0319	0.0239/0.0479
<i>R</i> ₁ / <i>wR</i> ₂ (all data) ^a	0.0244/0.0504	0.0154/0.0305	0.0353/0.0681	0.0201/0.0449	0.0179/0.0446	0.0129/0.0322	0.0316/0.0503
GOF (on <i>F</i> ²) ^a	1.054	1.088	1.025	1.073	1.199	1.048	1.071
largest diff peak and hole (e Å ⁻³)	+0.22/–0.16	+0.70/–0.50	+0.29/–0.23	+1.36/–1.51	+1.13/–0.80	+0.48/–0.35	+0.29/–0.34

$$^a R_1 = \Sigma(|F_o| - |F_c|) / \Sigma F_o; wR_2 = \{\Sigma[w(F_o^2 - F_c^2)^2] / \Sigma[w(F_o^2)^2]\}^{1/2}; GOF = \{\Sigma[w(F_o^2 - F_c^2)^2] / (n - p)\}^{1/2}.$$

population could be observed upon ligand coordination, a strong raise in electron population could be identified for the two normal NHC compounds **nIMI** and **1a** (Figure 11, b).

The heightened electron-donating capability of tetrazolyli-dene ligand **2** compared to normal tetrazolyli-dene ligand **1** was investigated by comparing changes in the Mulliken charges on all nitrogens of both ligands' heterocycles. Because of the 1,3-substitution pattern in **2** and the concomitant higher integration into the ligand's aromatic system, the N4 nitrogen atom adjacent to the carbene carbon is able to deliver a higher amount of electron density upon metal coordination than in the case of normal tetrazolyli-dene ligand **1** (Figure 12, see Supporting Information for details). While the Mulliken charge on N4 in ligand **1** gets lowered when the NHC is bound to Cr, the charge on N4 in ligand **2** is raised, suggesting loss of electrons. Interestingly, in contrast to N3 in **1**, N3 in **2** does not seem to be partaking in the electronic changes taking place during the process of metal bond formation. This observation reflects to some extent the expected heterocyclic system with local charges, proposed for **2** in Figure 1. Although this behavior is partly compensated by the heightened electron loss of N2 in **2**, over the whole heterocycle a higher electron loss can be observed.

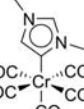
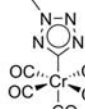
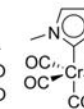
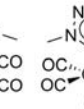
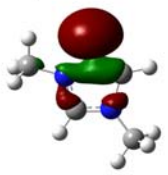
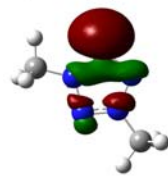
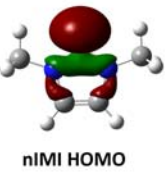
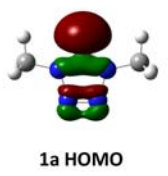
CONCLUSION

A selection of normal and abnormal tetrazolyli-dene complexes were synthesized and fully characterized. It was found that ligands with the normal 1,4-substitution show only limited stability compared to their abnormal congeners because of the tendency to release nitrogen from the backbone. To further elucidate the differences between the 1,3- and the 1,4-dimethyl-substituted NHC ligands, spectroscopic, crystallographic, and computational studies were undertaken. These investigations revealed pronounced variation arising from this seemingly simple change in substitution.

First, a variety of obtained spectroscopic data suggest that the abnormal tetrazolyli-dene **2** is a stronger electron donor than its normal congener **1**: (a) in ¹³C NMR of Ir COD complexes **1b** and **2b**, the olefin signals are shifted upfield for **2b**; (b) IR spectra and Raman spectra of Cr complexes **1a** and **2a** show for the ν (CO) vibrational bands an elevated average for **1a**; (c) IR spectra of **1c** and **2c** allow comparison of the two ligands to other donor ligands and reveal that abnormal tetrazolyli-dene **2** is comparable to ItBu, while normal tetrazolyli-dene **1** is analogous to P(iPr)₃ in donor strength.

Second, in crystallographic data, a slight trend observable in the Ir COD compounds **1b** and **2b** proposes a more alkyl-like character for the olefins in the metal complex coordinated to stronger σ -donor **1**. Interestingly, the metal carbene bond

Table 4. Results from of Calculated Structures of Methyl-Substituted NHC Ligands Bound to $\text{Cr}(\text{CO})_5$, Ordered from Left to Right by Decreasing Donor Strength^e

Calculate structure	Pivotal results from DFT calculations				Graphical representation of selected orbitals of the carbene fragments (carbene atom always on top)	
						
Name	aMI	2a	nMI	1a	aMI HOMO	2a HOMO
Distance $\text{C}_{\text{carbene}}-\text{Cr}^{\text{a}}$	2.117	2.075	2.125	2.091		
Mull. charge on $\text{C}_{\text{carbene}}^{\text{c}}$	0.109	0.281	0.297	0.335		
HOMO free carbene ^b	-0.124	-0.163	-0.154	-0.192		
HOMO complex ^b	-0.164	-0.181	-0.180	-0.198	nMI HOMO	1a HOMO
Ligand Bond Energy ^d	-67.416	-61.092	-59.574	-55.671		

^aDistances indicated in Angstrom [\AA]. ^bOrbital energies indicated in atomic units. ^cCharges indicated in electronic units. ^dEnergies indicated in kcal/mol; LBE calculated using general formula: $\text{LBE} = E_{\text{Complex}} - (E_{\text{Ligand}} + E_{\text{Cr-fragment}})$. ^eSince aMI was not reported to date, donor strength was estimated to be highest, based on observations made with this ligand class.^{5c}

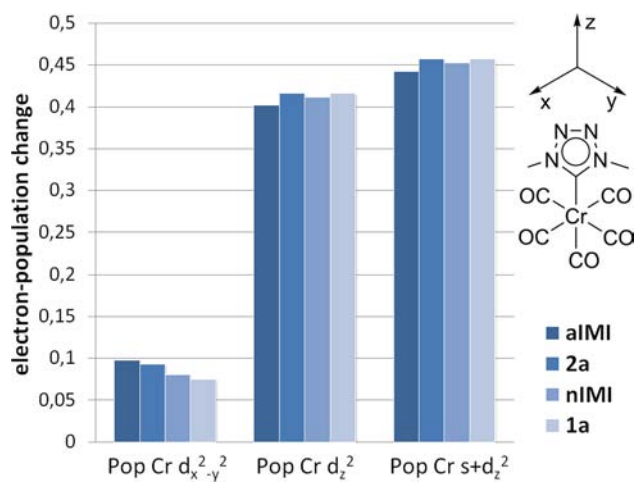


Figure 10. Graphical representation of the calculated population of selected Cr orbitals. Definition of axes used throughout the theoretical considerations.

distances are shortened in the Cr compounds **1a** and **2a** in comparison with the imidazolylidene or pyrazolylidene analogues.

Finally, computational data of abnormal and normal methyl-substituted imidazolylidene and tetrazolylidene complexes show that for carbene metal bond distances steric factors dominate electronic factors. For the examined complexes, a consistent trend of higher bond energies for stronger σ -donors was found. Furthermore it was discovered that the weaker σ -donating normal carbene ligands favor increasing metal to ligand π -backbonding contributions.

The focus of our ongoing investigations in this area lies on variation of ligand design to leverage stability for catalytic application.

EXPERIMENTAL SECTION

General Information. Manipulations were carried out under argon atmosphere, in a glovebox or using Schlenk techniques. Required glassware was flame-dried in vacuo prior to use. Solvents were dried with by a MBraun MB SPS apparatus and then degassed through repeated freeze–pump–thaw cycles. Commercially available compounds were used as received. Amberlite IRA-400 (Cl) Resin bought from SUPELCO was used for anion exchange of tetrazolium salts. NMR-spectra (^1H and ^{13}C) were recorded on a 400 MHz Bruker Avance III or a 400 MHz Bruker Avance DPX spectrometer at 298 K. The spectra were calibrated by using the residual solvent shifts as internal standards. Chemical shifts were referenced in parts per million (ppm). Abbreviations for signal multiplicities are as follows: singlet (s), doublet (d), triplet (t), quartet (q), multiplet (m), and broad (br). IR spectra were recorded on a Varian 670 FT-IR Spectrometer. Raman spectroscopy was performed on a Bio-Rad FT-Raman interferometer equipped with a Spectra-Physics Nd:YAG laser source (1064 nm, 500–700 mW) and a liquid-nitrogen-cooled Ge detector. ESI-HRMS analyses were performed on a Thermo Scientific LTQ Orbitrap XL by Thermo Fisher Scientific. Elemental analyses were conducted by the microanalytical laboratory of the TUM. Determination of dipole moments was carried out on a Slevogt (Weilheim) DM 01 dipolmeter. It should be noted that tetrazole based compounds are potential explosives and should be handled with appropriate care and safety equipment.

Single-Crystal X-ray Structure Determinations. Data were collected on an X-ray single-crystal diffractometer equipped with a CCD detector (APEX II, κ -CCD), a rotating anode (Bruker AXS, FR591) with Mo $K\alpha$ radiation ($\lambda = 0.71073 \text{ \AA}$) and a Montel-type focusing optic (compounds **1a**, **2a**, **2b**, **2c**, and **2d**) or a fine-focused sealed tube respectively (compounds **1b**, **1e**, and **2e**) and a graphite monochromator by using the SMART software package.²⁹ The measurements were performed on single crystals coated with perfluorinated ether. The crystals were fixed on the top of a glass fiber and transferred to the diffractometer. Crystals were frozen under a stream of cold nitrogen. A matrix scan was used to determine the initial lattice parameters. Reflections were merged and corrected for Lorenz and polarization effects, scan speed, and background using

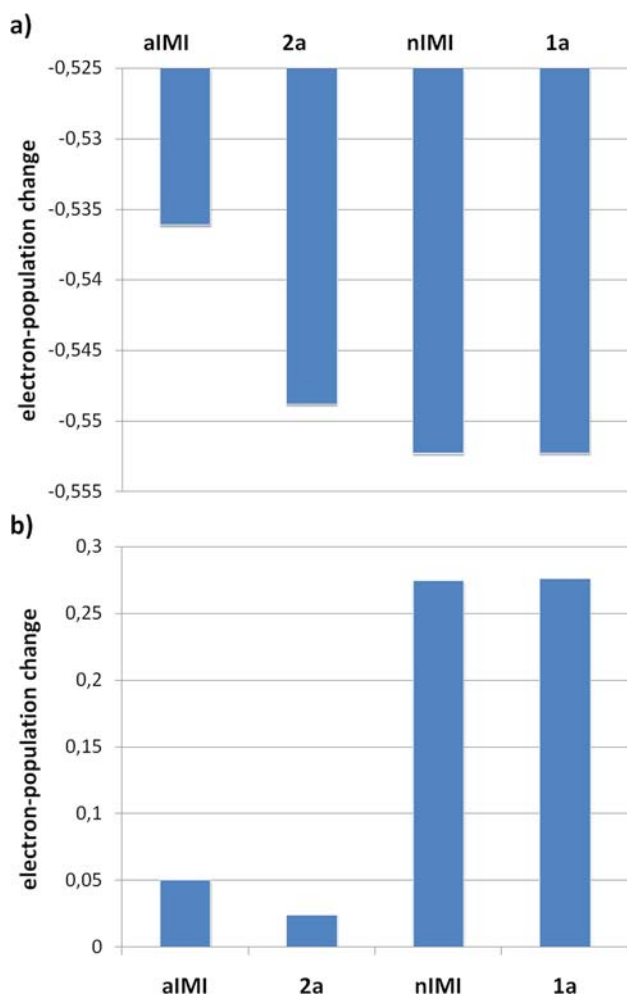


Figure 11. Graphical representation of the calculated changes in electron population in (a) $d_{xz} + d_{yz}$ -orbitals of Cr and (b) $p_x + p_y$ -orbitals of carbene carbon.

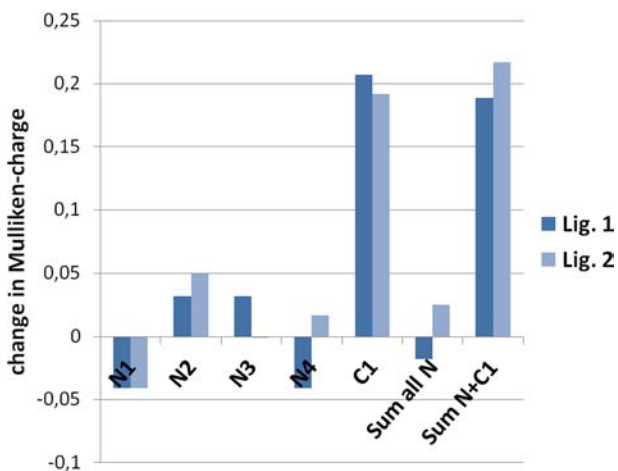


Figure 12. Graphical representation of changes in Mulliken-charge for all atoms of both ligands' heterocycles upon metal coordination. Positive values represent a growth in charge, hence higher electron donation of the respective atom.

SAINT.³⁰ Absorption corrections, including odd- and even-ordered spherical harmonics were performed using SADABS.³⁰ Space group assignments were based upon systematic absences, E statistics, and successful refinement of the structures. Structures were solved by

direct methods with the aid of successive difference Fourier maps, and were refined against all data using WinGX³¹ based on SIR-92³² (compound 2c) or the APEX 2 software²⁹ in conjunction with SHELXL-97³³ and SHELXL-97.³⁴ Unless otherwise noted, methyl hydrogen atoms were refined as part of rigid rotating groups, with a C–H distance of 0.98 Å and $U_{iso(H)} = 1.5 \cdot U_{eq(C)}$. Other H atoms were placed in calculated positions and refined using a riding model, with methylene and aromatic C–H distances of 0.99 and 0.95 Å, respectively, and $U_{iso(H)} = 1.2 \cdot U_{eq(C)}$. If not mentioned otherwise, non-hydrogen atoms were refined with anisotropic displacement parameters. Full-matrix least-squares refinements were carried out by minimizing $\sum w(F_o^2 - F_c^2)^2$ with SHELXL-97³³ weighting scheme. Neutral atom scattering factors for all atoms and anomalous dispersion corrections for the non-hydrogen atoms were taken from *International Tables for Crystallography*.³⁵ Images of the crystal structures were generated by PLATON.³⁶ For more and detailed information, see the Supporting Information. Crystallographic data (excluding structure factors) for the structures reported in this paper have been deposited with the Cambridge Crystallographic Data Centre as supplementary publication no. CCDC-926619 (1a), CCDC-926620 (1b), CCDC-926621 (2a), CCDC-926622 (2b), CCDC-926623 (2c), CCDC-926624 (2d), and CCDC-926625 (2e). Copies of the data can be obtained free of charge on application to CCDC, 12 Union Road, Cambridge CB2 1EZ, UK (fax: (+44)1223-336-033; e-mail: deposit@ccdc.cam.ac.uk).

Computational Details. All calculations have been performed with Gaussian09³⁷ by using the PBEPBE functional³⁸ together with the all electron basis set 6-31G*.³⁹ All optimized structures have been confirmed by frequency calculations to be true minima on the potential hyper surface. Frequency calculations have been used unscaled to characterize the CO vibrations to compare the bonding situations of the complexes. Dipole moments, Mulliken charges and orbital energies are taken from the population analysis by Mulliken⁴⁰ as implemented in Gaussian09. The MO representations of the “Mulliken orbitals” have been taken from cubegen calculations out of the checkpoint files from the optimized structures with a isolobal value of 0.01. NBO population analysis⁴¹ has been used for determining changes in the populations of natural orbitals of the ligand and the central atom on the way to the complex.

Synthetic Procedures. *Preparation of 1,4-Dimethyl-tetraazolium-tetrafluoroborate (1BF₄).* Under intense stirring, a solution of 5.00 g of 1-methyltetrazole (0.06 mol, 1.00 equiv) in 35 mL of dichloromethane was slowly added to 8.80 g of Me₃OBF₄ (0.06 mol, 1.00 equiv) in a 100 mL flask, which was externally cooled to 0 °C. After complete addition, the solution was stirred for 1.5 h at room temperature and then heated to reflux for 10 min. Precipitation of the product was accomplished by cooling the reaction mixture to –24 °C. After decantation of the mother liquor and washing the crystalline product with DCM at –24 °C, the solid was dried in vacuo. The obtained solid product mixture (10.8 g, 97%; containing ~90% 1,4-dimethyltetrazolium tetrafluoroborate and ~10% 1,3-dimethyltetrazolium tetrafluoroborate) was purified by recrystallization from ethanol to give 1BF₄ as colorless crystalline solid (8.40 g, 75.2%).

¹H NMR (400 MHz, DMSO-*d*₆): δ (ppm) = 10.93 (s, 1H, NCH), 4.33 (s, 6H, NCH₃). ¹³C NMR (101 MHz, DMSO-*d*₆): δ (ppm) = 143.50 (NCN), 37.37 (NCH₃). MS (FAB⁺) m/z (%): 99.1 [tetr]⁺ (100). MS (FAB⁻) m/z (%): 87.0 [BF₄]⁻ (70). MS (ESI⁺) m/z (%): 99.0 [tetr]⁺ (100). MS (ESI⁻) m/z (%): 87.0 [BF₄]⁻ (100).

Preparation of 1,3-Dimethyl-tetraazolium-tetrafluoroborate (2BF₄). Under intense stirring, a solution of 300 mg of 2-methyl-2H-tetrazol (3.58 mmol, 1.00 equiv) in 5 mL of dichloromethane was slowly added to 530 mg Me₃OBF₄ (3.58 mmol, 1.00 equiv) in 3 mL of dichloromethane in a 25 mL Schlenk tube, which was externally cooled to 0 °C. After complete addition, the solution was stirred for 1 h at room temperature and then heated to reflux for 10 min. Precipitation of the product was accomplished by reduction of the reaction solution in vacuo to 5 mL and cooling overnight at –30 °C. The mother liquor was decanted and the crystalline product was dried in vacuo (542 mg, 98.1%).

^1H NMR (400 MHz, D_2O): δ (ppm) = 9.90 (s, 1H, NCH), 4.73 (s, 3H, NCH_3), 4.50 (s, 3H, NCH_3). The compound was used in the subsequent step without further characterization.

Preparation of 1,4-Dimethyl-tetrazolium-chloride (1Cl). 1.00 g (5.38 mmol) of 1,4-dimethyl-tetrazolium-tetrafluoroborate was dissolved in 2 mL of deionized water and then passed through chloride charged anion exchange resin [Amberlite IRA-400 (Cl) Resin]. 20 mL of deionized water were added to flush down the anion chloride product. Removal of the solvent under vacuum gave a white hygroscopic solid (0.523 g, 72.2%) as product.

^1H NMR (400 MHz, $\text{DMSO}-d_6$): δ (ppm) = 11.27 (s, 1H, NCH), 4.34 (s, 6H, NCH_3). ^{13}C NMR (101 MHz, $\text{DMSO}-d_6$): δ (ppm) = 143.61 (NCN), 37.32 (NCH_3). MS (ESI) m/z (%): 99.0 [tetr^+] (100). HR-MS (ESI) m/z (%): calcd. for $\text{C}_3\text{H}_7\text{N}_4^+$ [tetr^+] 99.06652, found 99.06641(5).

Preparation of 1,3-Dimethyl-tetrazolium-chloride (2Cl). 1.00 g (5.38 mmol) of 1,3-dimethyl-tetrazolium-tetrafluoroborate was dissolved in 2 mL of deionized water and then passed through chloride charged anion exchange resin [Amberlite IRA-400 (Cl) Resin]. 20 mL of deionized water were added to flush down the anion exchange product. Removal of the solvent under vacuum gave a white hygroscopic solid (0.564 g, 87.9%) as product.

^1H NMR (400 MHz, CD_3CN): δ (ppm) = 10.66 (s, 1H, NCH), 4.59 (s, 3H, NCH_3), 4.45 (s, 3H, NCH_3). ^{13}C NMR (101 MHz, CD_3CN): δ (ppm) = 150.78 (NCN), 44.40 (NCH_3), 39.24 (NCH_3). MS (FAB $^+$) m/z (%): 99.0 [tetr^+] (100). MS (FAB $^-$) m/z (%): 35.3 [Cl^-] (25). MS (ESI) m/z (%): 99.0 [tetr^+] (100). HR-MS (ESI) m/z (%): calcd. for $\text{C}_3\text{H}_7\text{N}_4^+$ [tetr^+] 99.06652, found 99.06641(15); calcd. for $\text{C}_6\text{H}_4\text{ClN}_8^+$ [$2\text{tetr}^+ + \text{Cl}^-$] 233.10245, found 233.10228 (100).

Preparation of 1,4-Dimethyl-tetrazolyli-dene-chromium-pentacarbonyl (1a). 1a was synthesized following a previously published route^{9b} or according to the following procedure: Under argon atmosphere, 4.20 g of $\text{Na}_2[\text{Cr}_2(\text{CO})_{10}]$ (9.75 mmol, 1.00 equiv) were suspended in 15 mL of ethanol and a solution of 3.6 g of **1BF4** (19.3 mmol, 2.00 equiv) in 9 mL of water/ethanol (2:1) were added at -20°C . After the suspension changed color from yellow to orange, the solution was filtered and the orange solid was washed with ethanol (3×5 mL) and diethyl ether (2×5 mL) and dried in vacuo. The crystalline solid was dissolved in 15 mL of diglyme and under stirring and static vacuum heated to 100°C for 1 h. During this period, gas evolution and sublimation of $[\text{Cr}(\text{CO})_6]$ could be observed. After the mixture was cooled, the solvent was removed in vacuo and the residue was extracted with hexane (5×30 mL). The solvent of the extract was removed and the solid residue was purified by column chromatography [silica containing 5% H_2O ; after removal of a slightly fluorescent band with 100 mL hexane and 70 mL hexane/diethyl ether (3:1), the product was obtained as colorless band with hexane/diethyl ether (1:1)]. Removal of the solvents gave 0.80 g of 1a as colorless needles (25%).

^1H NMR (400 MHz, CDCl_3): δ (ppm) = 4.37 (s, 3H, NCH_3), 4.24 (s, 3H, NCH_3). ^{13}C NMR (101 MHz, CDCl_3): δ (ppm) = 221.98 (CO), 217.90 (CO), 200.91 (C_{tetra}), 40.79 (NCH_3), 38.11 (NCH_3). MS (CI) m/z (%): 290.0 [M^+] (100). IR (solid): $\nu(\text{cm}^{-1})$ = 2058, 1970, 1925, 1891, 1870 (C=O). EA: Anal. Calcd. for $\text{C}_8\text{H}_6\text{CrN}_4\text{O}_5$ (289.97) C, 33.12; H, 2.08; N, 19.31; Found C, 33.48; H, 2.08; N, 19.01.

Preparation of 1,3-Dimethyl-tetrazolyli-dene-chromium-pentacarbonyl (2a). Under stirring, a solution of 2.61 g (14.0 mmol, 1.00 equiv) in 5 mL of H_2O was at 0°C added to a suspension of 3.47 g of $\text{Na}_2[\text{Cr}_2(\text{CO})_{10}]$ (8.1 mmol, 0.60 equiv) in 10 mL of H_2O . The orange precipitate was filtered, washed with H_2O (4×5 mL) and dried at RT in vacuo. The solid residue was heated in static vacuo at 120°C for 1 h. During that time, the solid melted and showed intense gas development and colorless crystals could be collected at the cooling finger of the sublimation apparatus. After the mixture was cooled, the sublimate was extracted with 90 mL of diethyl ether/THF (2:1). The solid residue of the sublimation was extracted with 75 mL diethyl ether/THF (2:3). The collected organic extracts were combined and the solvent was removed in vacuo. Finally, the solid residue was purified by column chromatography (silica, containing 5%

H_2O ; after removal of the side product bands with 200 mL hexane/diethyl ether (1:1) the product could be obtained as light yellow band by flushing the silica with 600 mL diethyl ether]. Removal of the solvent gave 1.20 g (41%) of 2a as colorless prisms.

^1H NMR (400 MHz, CDCl_3): δ (ppm) = 4.27 (s, 6H, NCH_3). ^{13}C NMR (101 MHz, CDCl_3): δ (ppm) = 220.11 (CO), 216.50 (CO), 190.34 (C_{tetra}), 38.50 (NCH_3). MS (CI) m/z (%): 290.0 [M^+] (100), 262.0 [$\text{M} - \text{CO}$] (11). MS (ESI) m/z (%): 206.8 [$\text{M}-3\text{CO}$] (74). IR (solid): $\nu(\text{cm}^{-1})$ = 2056, 1949, 1910, 1882, 1854 (C=O). EA: Anal. Calcd. for $\text{C}_8\text{H}_6\text{CrN}_4\text{O}_5$ (289.97) C, 33.12; H, 2.08; N, 19.31; Found C, 33.24; H, 2.10; N, 19.03.

Preparation of 1,4-Dimethyl-tetrazolyli-dene-1,5-cyclooctadiene-irridium-chloride (1b). Under argon atmosphere, 8.0 mL of anhydrous acetone were added to a Schlenk tube charged with 1,4-dimethyl-tetrazolium-chloride (80.0 mg, 0.594 mmol, 1.00 equiv) and 1,5-cyclooctadiene-methoxy-irridium(I) dimer (197.0 mg, 0.297 mmol, 0.50 equiv). After stirring at room temperature for 18 h, the reaction mixture was filtered and all volatiles of the filtrate were removed in vacuo to give a yellow crude product. Extraction with anhydrous diethyl ether gave a yellow solid (87.0 mg, 33.7%) as product.

^1H NMR (400 MHz, CD_3CN): δ (ppm) = 4.68–4.53 (m, 2H, CCH), 4.20 (s, 6H, NCH_3), 3.21–2.98 (m, 2H, CCH), 2.25 (m, 4H, CCH_2), 1.89–1.77 (m, 2H, CCH_2), 1.74–1.55 (m, 2H, CCH_2). ^{13}C NMR (101 MHz, CD_3CN): δ (ppm) = 179.02 (C_{tetra}), 87.70 (CCH), 53.83 (CCH), 37.80 (NCH_3), 34.00 (CCH_2), 30.13 (CCH_2). MS (FAB) m/z (%): 433.5 [M^+] (36), 335.6 [$\text{M}-\text{tetra}^+$] (23). MS (ESI) m/z (%): 440.1 [$\text{M} - \text{Cl} + \text{MeCN}^+$] (100). EA: Anal. Calcd. for $\text{C}_{11}\text{H}_{18}\text{ClIrN}_4$ (434.08) C, 30.44; H, 4.18; N, 12.91. Found C, 30.46; H, 4.20; N, 10.90.

Preparation of 1,3-Dimethyl-tetrazolyli-dene-1,5-cyclooctadiene-irridium-chloride (2b). Under argon atmosphere, 8.0 mL of anhydrous acetone were added to a Schlenk tube charged with 1,3-dimethyl-tetrazolium-chloride (62.0 mg, 0.46 mmol, 1.00 equiv) and 1,5-cyclooctadiene-methoxy-irridium(I) dimer (155.0 mg, 0.23 mmol, 0.50 equiv). After stirring at room temperature for 18 h, the reaction mixture was filtered and the volume of the filtrate was reduced to 50%. Hexane was added and the solution was cooled to 4°C overnight to precipitate the product as a yellow solid (78 mg, 78%).

^1H NMR (400 MHz, CD_3CN): δ (ppm) = 4.45 (s, 2H, CCH), 4.29 (s, 3H, NCH_3), 4.27 (s, 3H, NCH_3), 3.27–3.01 (m, 2H, CCH), 2.35–2.13 (m, 4H, CCH_2), 1.83–1.73 (m, 2H, CCH_2), 1.70–1.53 (m, 2H, CCH_2). ^{13}C NMR (101 MHz, CD_3CN): δ (ppm) = 186.78 (C_{tetra}), 85.11 (CCH), 53.68 (CCH), 41.92 (NCH_3), 38.67 (NCH_3), 34.25 (CCH_2), 30.43 (CCH_2). MS (FAB) m/z (%): 433.5 [M^+] (20), 398.6 [$\text{M} - \text{Cl}^+$] (16). MS (ESI) m/z (%): 433.2 [M^+] (44). EA: Anal. Calcd. for $\text{C}_{11}\text{H}_{18}\text{ClIrN}_4$ (434.08): C, 30.44; H, 4.18; N, 12.91. Found: C, 30.42; H, 4.13; N, 12.61.

Preparation of 1,4-Dimethyl-tetrazolyli-dene-dicarbonyl-irridium-chloride (1c). Carbon monoxide was bubbled through a solution of 30.0 mg 1b (69.1 μmol) in 5 mL DCM for 15 min. During that period, the color of the reaction solution changed from orange-yellow to dark green. The reaction solution was filtered and all volatiles of the filtrate were removed in vacuo. The product was purified by column chromatography (silica, DCM, yellow band). Removal of the solvent gave 8.0 mg of 1c as yellow-brown solid (30%).

^1H NMR (400 MHz, CD_2Cl_2): δ (ppm) = 4.27 (s, 6H, NCH_3). ^{13}C NMR (101 MHz, CD_2Cl_2): δ (ppm) = 180.38 (CO), 173.11 (C_{tetra}), 167.56 (CO), 38.77 (NCH_3). MS (FAB) m/z (%): 382.5 [M^+] (100), 353.6 [$\text{M} - \text{CO}^+$] (69), 346.6 [$\text{M} - \text{Cl}^+$] (35). MS (CI) m/z (%): 382.5 [M^+] (100), 353.6 [$\text{M} - \text{CO}^+$] (20), 346.6 [$\text{M} - \text{Cl}^+$] (6). MS (ESI) m/z (%): 360.0 [$\text{M} - \text{N}_2^+$] (28), 344.0 [$\text{M} - \text{N}_2 - \text{CH}_3^+$] (38), 282.3 [$\text{M} - \text{tetra}^+$] (100). IR (CH_2Cl_2): $\nu(\text{cm}^{-1})$ = 2076, 1989 (C=O). EA: Anal. Calcd. for $\text{C}_3\text{H}_6\text{ClIrN}_4\text{O}_2$ (381.98) C, 15.73; H, 1.58; N, 14.67. Found C, 15.99; H, 1.51; N, 14.33.

Preparation of 1,3-Dimethyl-tetrazolyli-dene-dicarbonyl-irridium-chloride (2c). Carbon monoxide was bubbled through a solution of 50.0 mg of 2b (115 μmol) in 10 mL of toluene for 15 min. During that period, the color of the reaction solution changed from orange-yellow to light yellow. After 15 min, carbon monoxide addition was stopped, and the reaction mixture was stirred at RT under CO atmosphere.

After another 15 min, the solvent was reduced in vacuo to ~3 mL and 20 mL of hexane were added to precipitate a fine yellow-greenish solid of **2c**, which was washed with hexane (2 × 15 mL) and dried in vacuo (25.0 mg, 57%).

¹H NMR (400 MHz, CD₂Cl₂): δ (ppm) = 4.46 (s, 3H, NCH₃), 4.34 (s, 3H, NCH₃). ¹³C NMR (101 MHz, CD₂Cl₂): δ (ppm) = 182.07 (C_{tetra}), 181.57 (CO), 168.74 (CO), 42.24 (NCH₃), 39.38 (NCH₃). MS (FAB) *m/z* (%): 382.5 [M]⁺ (66), 353.6 [M - CO]⁺ (41), 346.6 [M - Cl]⁺ (22). MS (ESI) *m/z* (%): 388.0 [M - Cl + MeCN]⁺ (65), 360.0 [M - Cl - CO + MeCN]⁺ (45). IR (CH₂Cl₂): ν (cm⁻¹) = 2063, 1981 (C=O). EA: Anal. Calcd. for C₅H₆ClIrN₄O₂ (381.98) C, 15.73; H, 1.58; N, 14.67. Found C, 16.22; H, 1.69; N, 14.25.

Preparation of 1,4-Dimethyl-tetrazolylidene-silver-chloride (1d). Under argon atmosphere, 2 × 5 mL of anhydrous acetonitrile were added to two separate Schlenk tubes charged with 1,4-dimethyl-tetrazolium-chloride (100.0 mg, 0.743 mmol, 1.00 equiv) and silver oxide (0.517 g, 2.23 mmol, 3.00 equiv). The solution containing the tetrazolium salt was added to the Ag₂O suspension at -20 °C. The reaction mixture was stirred under exclusion of light for 16 h and was slowly warmed up to room temperature. Then, the reaction mixture was filtered through Celite, and the filtrate was concentrated. 5 mL of anhydrous diethyl ether were added to precipitate a white solid (26.0 mg, 15.1%) as product.

¹H NMR (400 MHz, CD₃CN): δ (ppm) = 4.27 (s, 6H, NCH₃). MS (FAB) *m/z* (%): 303.0 [M + tetra]⁺ (96), 206.9 [M - Cl]⁺ (22). MS (ESI) *m/z* (%): 190.8 [M - CH₂]⁺ (94).

Preparation of 1,3-Dimethyl-tetrazolylidene-silver-chloride (2d). Under argon atmosphere, 20 mL of anhydrous dichloromethane were added to a Schlenk tube charged with 1,3-dimethyl-tetrazolium-chloride (100.0 mg, 0.743 mmol, 1.00 equiv) and silver oxide (172.0 mg, 0.743 mmol, 1.00 equiv). The reaction mixture was stirred at room temperature under exclusion of light for 4 h. Then, the reaction mixture was filtered through Celite and the filtrate was concentrated. 8 mL of anhydrous hexane were added to give a white solid (108.0 mg, 60.2%) as product.

¹H NMR (400 MHz, CD₂Cl₂): δ (ppm) = 4.51 (s, 3H, NCH₃), 4.29 (s, 3H, NCH₃). ¹³C NMR (101 MHz, DMSO-*d*₆): δ (ppm) = 182.40 (C_{tetra}), 41.14 (NCH₃), 38.15 (NCH₃). MS (FAB) *m/z* (%): 206.7 [M - Cl]⁺ (51). MS (ESI) *m/z* (%): 245.9 [M - Cl + MeCN]⁺ (100), 204.0 [M - Cl]⁺ (56). EA: Anal. Calcd. for C₃H₆AgClN₄ (239.93): C, 14.92; H, 2.50; N, 23.21. Found: C, 15.37; H, 2.55; N, 22.90.

Preparation of Bis-1,4-dimethyl-tetrazolylidene-silver-tetrafluoroborate (1e). Under argon atmosphere, 15 mL of anhydrous acetonitrile were added to two separate Schlenk tubes charged with 1,4-dimethyl-tetrazolium-tetrafluoroborate (182.0 mg, 0.979 mmol, 1.00 equiv) and silver oxide (113 mg, 0.489 mmol, 0.50 equiv). The solution containing the tetrazolium salt was added to the Ag₂O suspension at -20 °C. After 7 h of stirring under exclusion of light, the reaction mixture was slowly warmed up to room temperature. Then, the reaction mixture was filtered through Celite and the filtrate was concentrated. 10 mL of anhydrous diethyl ether were added to precipitate a white solid (208.0 mg, 53.3%) as product.

¹H NMR (400 MHz, CD₃CN): δ (ppm) = 4.25 (s, 6H, NCH₃). ¹³C NMR (101 MHz, CD₃CN): δ (ppm) = 176.79 (C_{tetra}), 38.77 (NCH₃). MS (FAB⁺) *m/z* (%): 303.0 [M⁺] (100). MS (FAB⁻) *m/z* (%): 86.9 [BF₄⁻] (100). MS (ESI⁺) *m/z* (%): 694.7 [2 M + BF₄]⁺ (1), 302.8 [M]⁺ (11), 188.9 [M - Tetr-CH₄]⁺ (100). MS (ESI⁻) *m/z* (%): 87.0 [BF₄⁻] (100).

Preparation of 1,3-Dimethyl-tetrazolylidene-Cp-molybdenum-dicarbonyl-chloride (2e). Under argon atmosphere, 3 mL of anhydrous dichloromethane were added to Schlenk tube charged with 1,3-dimethyl-tetrazolylidene-silver-chloride (50.0 mg, 0.207 mmol, 1.00 equiv) and [Mo(CO)₂ClCp] (58.0 mg, 0.207 mmol, 1.00 equiv). The slurry was heated to reflux for 5 h under exclusion of light. Subsequently, the reaction mixture was filtered through Celite to give a dark red solution. After concentrating the filtrate, 5 mL of anhydrous hexane were added to give a red precipitate as crude product. A red solid (0.033 g, 45.7%) was obtained by recrystallization from dichloromethane and hexane.

¹H NMR (400 MHz, CD₂Cl₂): δ (ppm) = 5.61 (s, 5H, H_{cp}), 4.36 (s, 3H, NCH₃), 4.07 (s, 3H, NCH₃). ¹³C NMR (101 MHz, CD₂Cl₂): δ (ppm) = 260.48 (CO), 253.20 (CO), 196.72 (C_{tetra}), 96.83 (C_{cp}), 41.47 (NCH₃), 38.63 (NCH₃). MS (ESI) *m/z* (%): 357.8 [M - Cl + MeCN]⁺ (5). IR (solid): ν (cm⁻¹) = 1940, 1844 (C=O). EA: Anal. Calcd. for C₁₀H₁₁ClMoN₄O₂ (351.96) C, 34.25; H, 3.16; N, 15.98; Found C, 34.35; H, 3.23; N, 16.17.

■ ASSOCIATED CONTENT

Supporting Information

Tables of crystal parameters, atomic coordinates, bond lengths, bond angles, and thermal displacement parameters for **1a**, **1b**, **2a**, **2b**, **2c**, **2d**, and **2e** in .cif format, as well as data for **1e**, for which the residual electron density is too high for further analysis, NMR spectra, as well as detailed crystallographic information. This material is available free of charge via the Internet at <http://pubs.acs.org>.

■ AUTHOR INFORMATION

Corresponding Author

*E-mail: fritz.kuehn@ch.tum.de.

Author Contributions

[†]Equally contributing coauthors.

Notes

The authors declare no competing financial interest.

■ ACKNOWLEDGMENTS

The authors thank the TUM graduate school and the Bavarian Network of Excellence NANOCAT for financial support. M.D. thanks the Leibniz-Computing Center (LRZ) of the Bavarian Academy of Sciences for computational time and resources.

■ REFERENCES

- (a) Öfele, K. J. *Organomet. Chem.* **1968**, *12*, P42. (b) Wanzlick, H. W.; Schönherr, H. J. *Angew. Chem., Int. Ed.* **1968**, *7*, 141. (c) Arduengo III, A. J. U.S. Patent 5077414, 1991.
- (a) Herrmann, W. A. *Angew. Chem., Int. Ed.* **2002**, *41*, 1290. (b) Lin, J. C. Y.; Huang, R. T. W.; Lee, C. S.; Bhattacharyya, A.; Hwang, W. S.; Lin, I. J. B. *Chem. Rev.* **2009**, *109*, 3561. (c) Arnold, P. L.; Casely, I. J. *Chem. Rev.* **2009**, *109*, 3599. (d) Díez-González, S.; Marion, N.; Nolan, S. P. *Chem. Rev.* **2009**, *109*, 3612. (e) Hindi, K. M.; Panzner, M. J.; Tessier, C. A.; Cannon, C. L.; Youngs, W. J. *Chem. Rev.* **2009**, *109*, 3859. (f) Samojłowicz, C.; Bieniek, M.; Grela, K. *Chem. Rev.* **2009**, *109*, 3708. (g) Burtscher, D.; Grela, K. *Angew. Chem., Int. Ed.* **2009**, *48*, 442. (h) Dröge, T.; Glorius, F. *Angew. Chem., Int. Ed.* **2010**, *49*, 6940. (i) Glorius, F. In *N-Heterocyclic Carbenes in Transition Metal Catalysis*; Glorius, F., Ed.; Springer: Berlin, 2007; Vol. 21, p 1. (j) Briel, O.; Cazin, C. S. J. In *N-Heterocyclic Carbenes in Transition Metal Catalysis and Organocatalysis*; Cazin, C. S. J., Ed.; Springer: Dordrecht, the Netherlands: 2011, p 315. (k) Schaper, L.-A.; Hock, S. J.; Herrmann, W. A.; Kühn, F. E. *Angew. Chem., Int. Ed.* **2013**, *52*, 270.
- (a) Öfele, K.; Herrmann, W. A.; Mihalios, D.; Elison, M.; Herdtweck, E.; Scherer, W.; Mink, J. J. *Organomet. Chem.* **1993**, *459*, 177. (b) Herrmann, W. A.; Elison, M.; Fischer, J.; Köcher, C.; Öfele, K. U.S. Patent 5728839, 1998. (c) Herrmann, W. A.; Elison, M.; Fischer, J.; Köcher, C.; Artus, G. R. J. *Angew. Chem., Int. Ed.* **1995**, *34*, 2371. (d) Wanzlick, H.-W.; Schikora, E. *Chem. Ber.* **1961**, *94*, 2389.
- 5217 references were found for the keyword "N-heterocyclic carbene", when entered in a Scifinder "Research Topic" search (Scifinder online version), CAS, <https://scifinder.cas.org> (accessed Feb 10, 2013).
- (a) Gründemann, S.; Kovacevic, A.; Albrecht, M.; Faller Robert, J. W.; Crabtree, H. *Chem. Commun.* **2001**, 2274. (b) Gründemann, S.; Kovacevic, A.; Albrecht, M.; Faller, J. W.; Crabtree, R. H. *J. Am. Chem. Soc.* **2002**, *124*, 10473. (c) Chianese, A. R.; Kovacevic, A.; Zeglis, B. M.; Faller, J. W.; Crabtree, R. H. *Organometallics* **2004**, *23*, 2461.

- (d) Schuster, O.; Yang, L.; Raubenheimer, H. G.; Albrecht, M. *Chem. Rev.* **2009**, *109*, 3445.
- (6) (a) Mathew, P.; Neels, A.; Albrecht, M. *J. Am. Chem. Soc.* **2008**, *130*, 13534. (b) Donnelly, K. F.; Petronilho, A.; Albrecht, M. *Chem. Commun.* **2013**, 1145.
- (7) Schaper, L.-A.; Öfele, K.; Kadyrov, R.; Bechlars, B.; Drees, M.; Cokoja, M.; Herrmann, W. A.; Kühn, F. E. *Chem. Commun.* **2012**, 3857.
- (8) (a) Öfele, K.; Kreiter, C. G. *Chem. Ber.* **1972**, *105*, 529. (b) Müller, J.; Öfele, K.; Krebs, G. *J. Organomet. Chem.* **1974**, *82*, 383.
- (9) (a) Herrmann, W. A.; Schütz, J.; Frey, G. D.; Herdtweck, E. *Organometallics* **2006**, *25*, 2437. (b) Frey, G. D.; Öfele, K.; Krist, H. G.; Herdtweck, E.; Herrmann, W. A. *Inorg. Chim. Acta* **2006**, *359*, 2622.
- (10) Bortenschlager, M.; Schütz, J.; von Preysing, D.; Nuyken, O.; Herrmann, W. A.; Weberskirch, R. *J. Organomet. Chem.* **2005**, *690*, 6233.
- (11) Gabrielli, W. F.; Nogai, S. D.; McKenzie, J. M.; Cronje, S.; Raubenheimer, H. G. *New J. Chem.* **2009**, *33*, 2208.
- (12) Araki, S.; Wanibe, Y.; Uno, F.; Morikawa, A.; Yamamoto, K.; Chiba, K.; Butsugan, Y. *Chem. Ber.* **1993**, *126*, 1149.
- (13) Araki, S.; Yokoi, K.; Sato, R.; Hirashita, T.; Setsune, J.-I. *J. Heterocycl. Chem.* **2009**, *46*, 164.
- (14) Wang, H. M. J.; Lin, I. J. B. *Organometallics* **1998**, *17*, 972.
- (15) Müller, J.; Öfele, K.; Krebs, G. *J. Organomet. Chem.* **1974**, *82*, 383.
- (16) Li, S.; Kee, C. W.; Huang, K.-W.; Hor, T. S. A.; Zhao, J. *Organometallics* **2010**, *29*, 1924.
- (17) (a) Kelly, R. A., III; Clavier, H.; Giudice, S.; Scott, N. M.; Stevens, E. D.; Bordner, J.; Samardjiev, I.; Hoff, C. D.; Cavallo, L.; Nolan, S. P. *Organometallics* **2007**, *27*, 202. (b) Huynh, H. V.; Han, Y.; Jothibasu, R.; Yang, J. A. *Organometallics* **2009**, *28*, 5395.
- (18) (a) Hartwig, J. F. In *Organotransition Metal Chemistry: From Bonding to Catalysis*; University Science Books: Sausalito, CA, 2010, p 51; (b) Brück, A.; Gallego, D.; Wang, W.; Irran, E.; Driess, M.; Hartwig, J. F. *Angew. Chem., Int. Ed.* **2012**, *51*, 11478.
- (19) Tolman, C. A. *Chem. Rev.* **1977**, *77*, 313.
- (20) Mink, J.; Goggin, P. L. *Can. J. Chem.* **1991**, *69*, 1857.
- (21) Tafipolsky, M.; Scherer, W.; Öfele, K.; Artus, G.; Pedersen, B.; Herrmann, W. A.; McGrady, G. S. *J. Am. Chem. Soc.* **2002**, *124*, 5865.
- (22) (a) Herrmann, W. A.; Roesky, P. W.; Elison, M.; Artus, G.; Öfele, K. *Organometallics* **1995**, *14*, 1085. (b) Nonnenmacher, M.; Kunz, D.; Rominger, F.; Oesser, T. *J. Organomet. Chem.* **2005**, *690*, 5647. (c) Hahn, F. E.; Langenhahn, V.; Meier, N.; Lügger, T.; Fehlhammer, W. P. *Chem.—Eur. J.* **2003**, *9*, 704. (d) Bolm, C.; Kesselgruber, M.; Raabe, G. *Organometallics* **2002**, *21*, 707. (e) Sakurai, H.; Sugitani, K.; Moriuchi, T.; Hirao, T. *J. Organomet. Chem.* **2005**, *690*, 1750. (f) Majhi, P. K.; Sauerbrey, S.; Schnakenburg, G.; Arduengo, A. J.; Streubel, R. *Inorg. Chem.* **2012**, *51*, 10408.
- (23) (a) Leuthäuser, S.; Schwarz, D.; Plenio, H. *Chem.—Eur. J.* **2007**, *13*, 7195. (b) Metallinos, C.; Du, X. *Organometallics* **2009**, *28*, 1233. (c) Zinner, S. C.; Rentzsch, C. F.; Herdtweck, E.; Herrmann, W. A.; Kühn, F. E. *Dalton Trans.* **2009**, 7055.
- (24) (a) Su, H.-L.; Pérez, L. M.; Lee, S.-J.; Reibenspies, J. H.; Bazzi, H. S.; Bergbreiter, D. E. *Organometallics* **2012**, *31*, 4063. (b) Gimeno, M. C.; Laguna, A.; Visbal, R. *Organometallics* **2012**, *31*, 7146. (c) de Frémont, P.; Scott, N. M.; Stevens, E. D.; Ramnial, T.; Lightbody, O. C.; Macdonald, C. L. B.; Clyburne, J. A. C.; Abernethy, C. D.; Nolan, S. P. *Organometallics* **2005**, *24*, 6301.
- (25) (a) Lee, M.-T.; Hu, C.-H. *Organometallics* **2004**, *23*, 976. (b) Lai, C.-L.; Guo, W.-H.; Lee, M.-T.; Hu, C.-H. *J. Organomet. Chem.* **2005**, *690*, 5867. (c) Tonner, R.; Heydenrych, G.; Frenking, G. *Chem. Asian J.* **2007**, *2*, 1555.
- (26) (a) Hu, X.; Castro-Rodriguez, I.; Olsen, K.; Meyer, K. *Organometallics* **2004**, *23*, 755. (b) Boehme, C.; Frenking, G. *Organometallics* **1998**, *17*, 5801. (c) Benitez, D.; Shapiro, N. D.; Tkatchouk, E.; Wang, Y.; Goddard, W. A.; Toste, F. D. *Nature Chem.* **2009**, *1*, 482. (d) Sanderson, M. D.; Kamplain, J. W.; Bielawski, C. W. *J. Am. Chem. Soc.* **2006**, *128*, 16514.
- (27) Jacobsen, H.; Correa, A.; Costabile, C.; Cavallo, L. *J. Organomet. Chem.* **2006**, *691*, 4350.
- (28) Xu, X.; Kim, S. H.; Zhang, X.; Das, A. K.; Hirao, H.; Hong, S. H. *Organometallics* **2012**, *32*, 164.
- (29) APEX suite of crystallographic software. APEX 2, version 2008.4; Bruker AXS Inc.: Madison, WI, U.S.A., 2008.
- (30) SAINT, version 7.56a; SADABS, version 2008/1; Bruker AXS Inc.: Madison, WI, U.S.A., 2008.
- (31) Farrugia, L. J. *J. Appl. Crystallogr.* **1999**, *32*, 837.
- (32) (a) Altomare, A.; Burla, M. C.; Camalli, M.; Casciarano, G. L.; Giacovazzo, C.; Guagliardi, A.; Moliterni, A. G. G.; Polidori, G.; Spagna, R. *J. Appl. Crystallogr.* **1999**, *32*, 115. (b) Sheldrick, G. M., *SHELXS-97, Program for Crystal Structure Solution*; University of Göttingen: Göttingen, Germany, 1997.
- (33) Sheldrick, G. M. *SHELXL-97*; University of Göttingen: Göttingen, Germany, 1998.
- (34) Hübschle, C. B.; Sheldrick, G. M.; Dittrich, B. *J. Appl. Crystallogr.* **2011**, *44*, 1281.
- (35) Wilson, A. J. C., Ed.; *International Tables for Crystallography*; Kluwer Academic Publishers: Dordrecht, the Netherlands, 1992.
- (36) Spek, A. L. *PLATON, A Multipurpose Crystallographic Tool*; Utrecht University: Utrecht, the Netherlands, 2010.
- (37) Frisch, M. J.; Trucks, G. W.; Schlegel, H. B.; Scuseria, G. E.; Robb, M. A.; Cheeseman, J. R.; Scalmani, G.; Barone, V.; Mennucci, B.; Petersson, G. A.; Nakatsuji, H.; Caricato, M.; Li, X.; Hratchian, H. P.; Izmaylov, A. F.; Bloino, J.; Zheng, G.; Sonnenberg, J. L.; Hada, M.; Ehara, M.; Toyota, K.; Fukuda, R.; Hasegawa, J.; Ishida, M.; Nakajima, T.; Honda, Y.; Kitao, O.; Nakai, H.; Vreven, T.; Montgomery, J. A., Jr.; Peralta, J. E.; Ogliaro, F.; Bearpark, M.; Heyd, J. J.; Brothers, E.; Kudin, K. N.; Staroverov, V. N.; Kobayashi, R.; Normand, J.; Raghavachari, K.; Rendell, A.; Burant, J. C.; Iyengar, S. S.; Tomasi, J.; Cossi, M.; Rega, N.; Millam, J. M.; Klene, M.; Knox, J. E.; Cross, J. B.; Bakken, V.; Adamo, C.; Jaramillo, J.; Gomperts, R.; Stratmann, R. E.; Yazyev, O.; Austin, A. J.; Cammi, R.; Pomelli, C.; Ochterski, J. W.; Martin, R. L.; Morokuma, K.; Zakrzewski, V. G.; Voth, G. A.; Salvador, P.; Dannenberg, J. J.; Dapprich, S.; Daniels, A. D.; Farkas, O.; Foresman, J. B.; Ortiz, J. V.; Cioslowski, J.; Fox, D. J. *Gaussian 09*, revision C.2; Gaussian, Inc.: Wallingford, CT, 2009.
- (38) (a) Perdew, J. P.; Burke, K.; Ernzerhof, M. *Phys. Rev. Lett.* **1996**, *77*, 3865. (b) Perdew, J. P.; Burke, K.; Ernzerhof, M. *Phys. Rev. Lett.* **1997**, *78*, 1396.
- (39) (a) Ditchfield, R.; Hehre, W. J.; Pople, J. A. *J. Chem. Phys.* **1971**, *54*, 724. (b) Hehre, W. J.; Ditchfield, R.; Pople, J. A. *J. Chem. Phys.* **1972**, *56*, 2257. (c) Hariharan, P. C.; Pople, J. A. *Theor. Chim. Acta* **1973**, *28*, 213. (d) Francl, M. M.; Pietro, W. J.; Hehre, W. J.; Binkley, J. S.; DeFrees, D. J.; Pople, J. A.; Gordon, M. S. *J. Chem. Phys.* **1982**, *77*, 3654.
- (40) Mulliken, R. S. *J. Chem. Phys.* **1955**, *23*, 1833.
- (41) (a) Foster, J. P.; Weinhold, F. *J. Am. Chem. Soc.* **1980**, *102*, 7211. (b) Reed, A. E.; Weinstock, R. B.; Weinhold, F. *J. Chem. Phys.* **1985**, *83*, 735. (c) Reed, A. E.; Curtiss, L. A.; Weinhold, F. *Chem. Rev.* **1988**, *88*, 899.